Interface-Resolved Simulation of Droplet Evaporation

METIN MURADOGLU
Department of Mechanical Engineering, Koc University, Istanbul, Turkey.
E-mail: mmuradoglu@ku.edu.tr

Outline

- Surface Phenomena and Multiphase Flows
- Front-Tracking Method
- Droplet Evaporation and Burning
  - Numerical Treatment of Phase Change
  - Validation
  - Droplet evaporation and burning
  - Droplet evaporation in convective environment
  - Performance evaluation of low-order models
- Viscoelasticity & Surfactant
- Conclusions

Surface Tension and Interfacial Phenomena

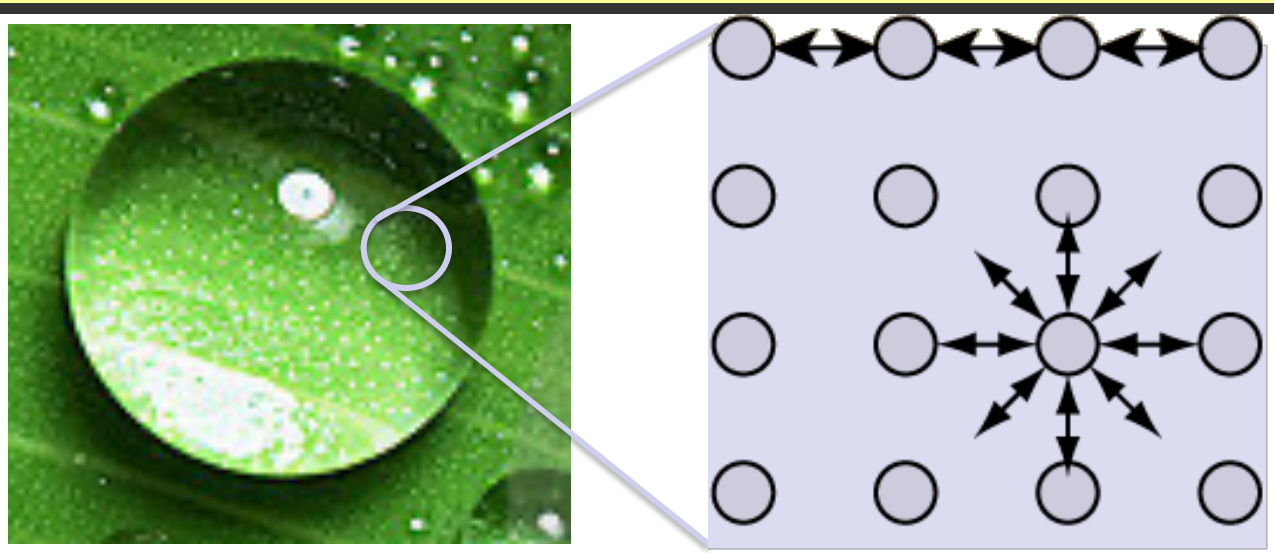

- The 'unhappy' molecules cause **tension** at the interface
- Tries to minimize the surface area
- Becomes significant as size gets smaller

$$\frac{\text{Surface Force}}{\text{Volume Force}} \sim \frac{\text{Area}}{\text{Volume}} \sim \frac{1}{R} \to \infty \quad \text{as} \quad R \to 0$$

- Responsible for a wide range of natural phenomena

Examples

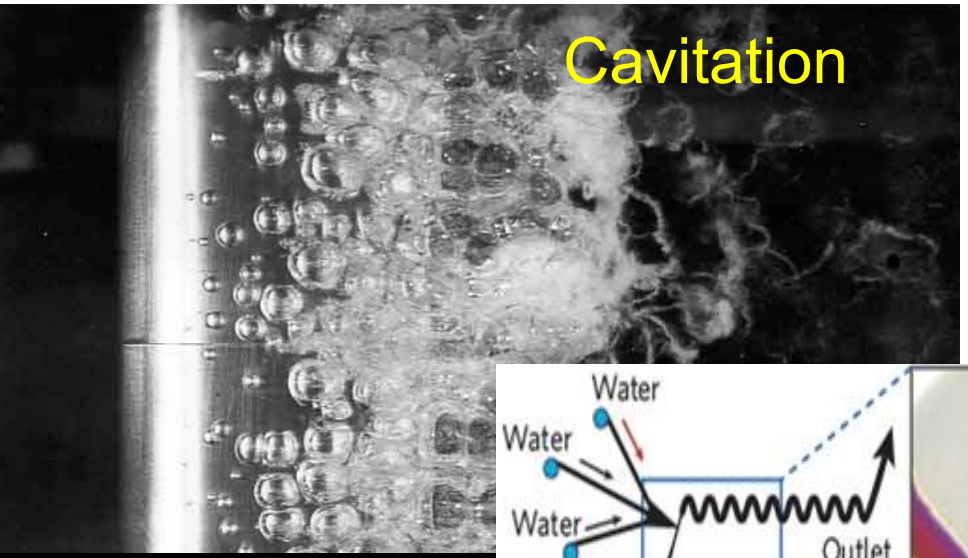
Cavitation

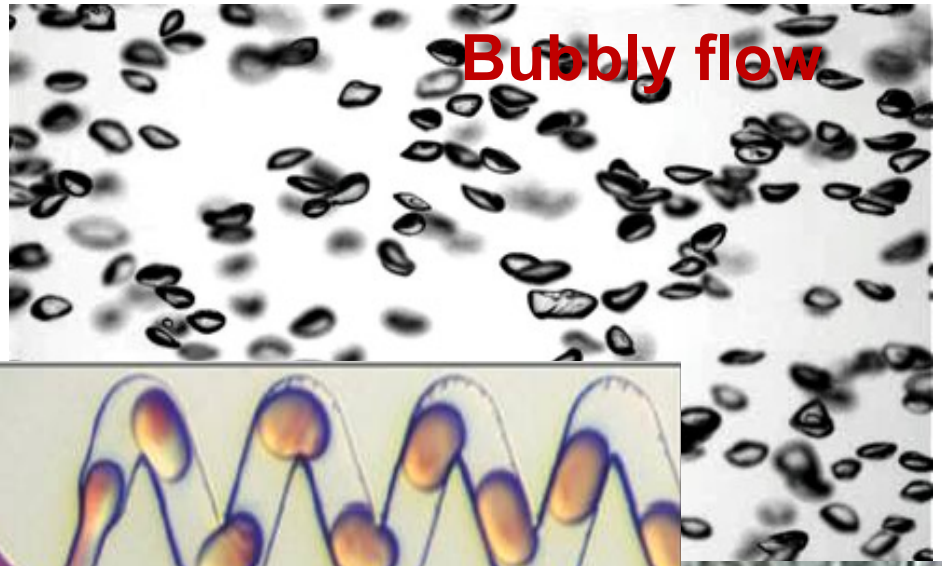
Bubbly flow

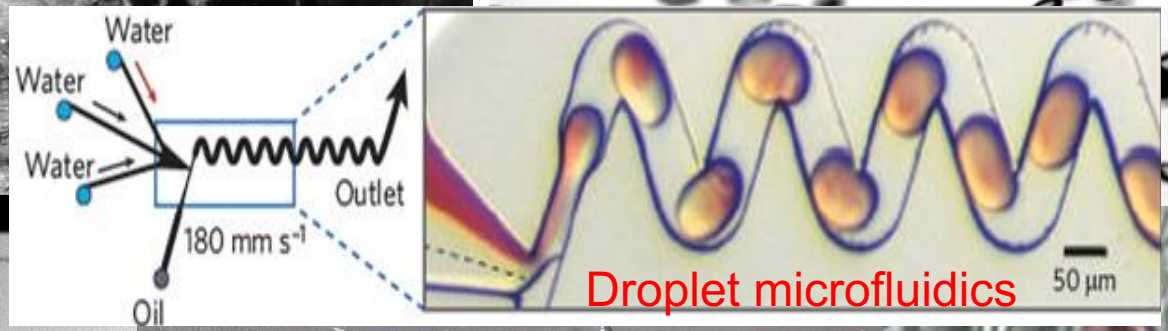
Water
Water
Water
Outlet
180 mm s-1
Oil
Droplet microfluidics
50 µm

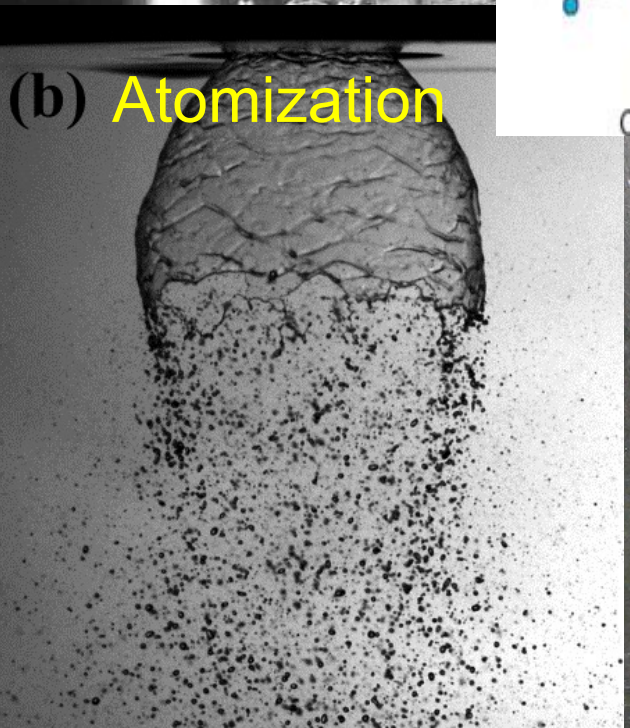
(b) Atomization

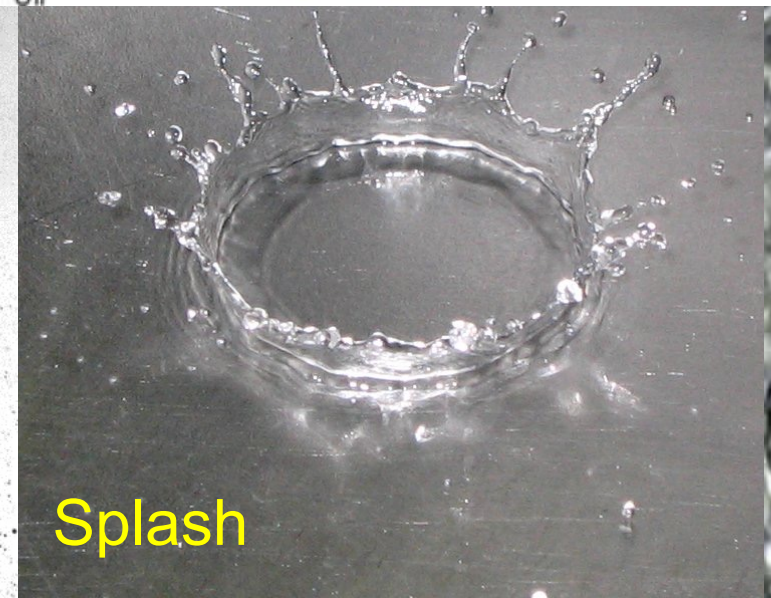
Splash


10 µm
Blood cells

Multiphase Systems

Flow systems composed of immiscible phases and fluids, separated by a sharp interface moving and deforming with flow.

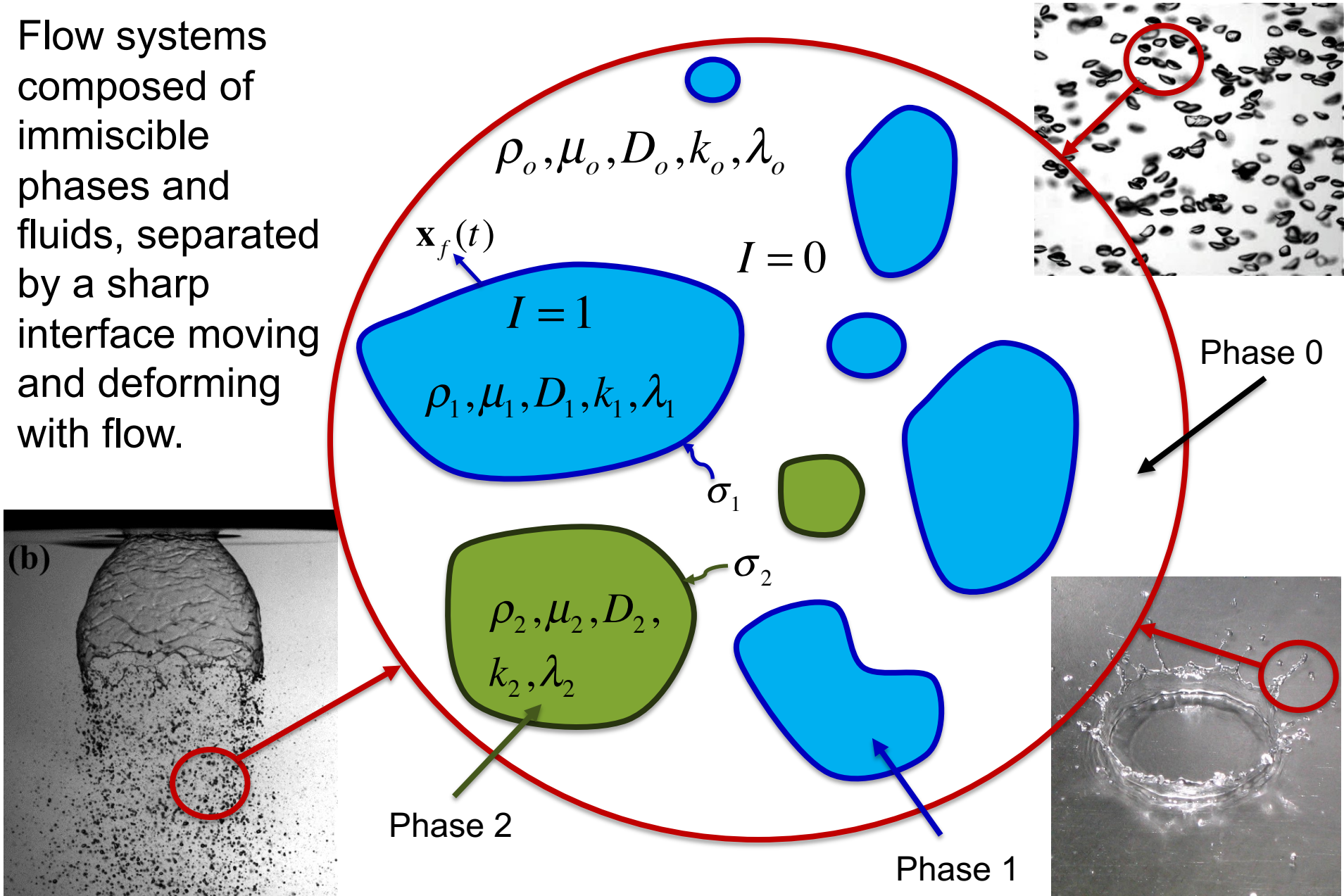

Multiphase Flows: Particle-Resolved Simulations

Common Features:

- Several phases flow together
- Phases are separated by a moving and deforming interface
- The physics is well described by the continuum theories
- Properties change discontinuously across the interface
- Fluids may be Newtonian or Non-Newtonian
- Fluids are assumed to be incompressible
- Full flow equations are solved numerically inside and outside the drop

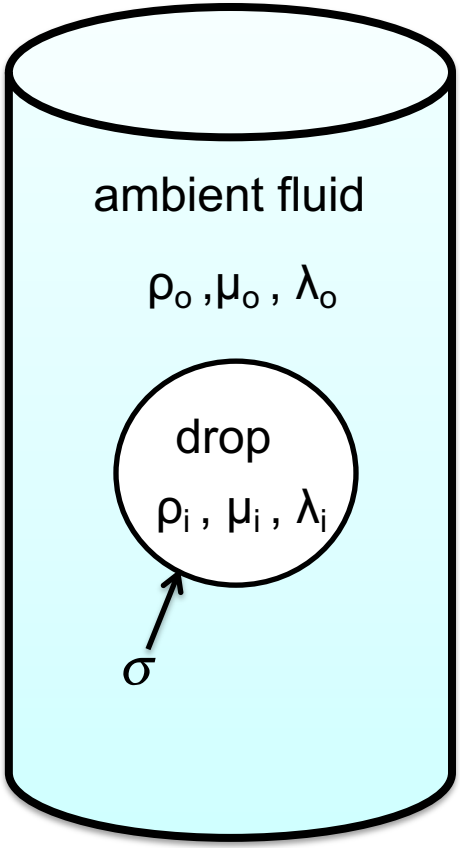

Mean Free Path (Deen, 1998)
Liquids ~ 0.3 nm
Gases ~ 100 nm

Mathematical Formulation

Flow equations: One-Field Formulation

$$\frac{\partial \boldsymbol{u}}{\partial t} + \nabla \cdot (\rho \boldsymbol{u}\boldsymbol{u}) = -\nabla p + \nabla \cdot \mu(\nabla \boldsymbol{u} + \nabla^T \boldsymbol{u}) + \boldsymbol{g}\Delta\rho + \boxed{\int_A \left(\sigma(\Gamma)\kappa \boldsymbol{n} + \nabla_s \sigma(\Gamma)\right)\delta\left(\boldsymbol{x} - \boldsymbol{x}_f\right) dA}$$

$$\nabla \cdot \boldsymbol{u} = 0$$

Body force due to surface tension

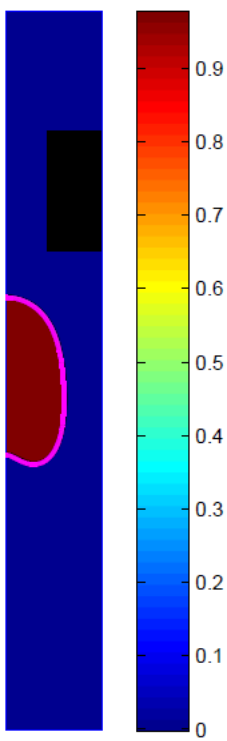

Define an indicator function:

$$I = \begin{cases} 1 & \text{inside} \\ 0 & \text{outside} \end{cases}$$

Set the material properties everywhere:

$$\rho = I\rho_i + (1 - I)\rho_o$$

$$\mu = I\mu_i + (1 - I)\mu_o$$

Front-Tracking Method

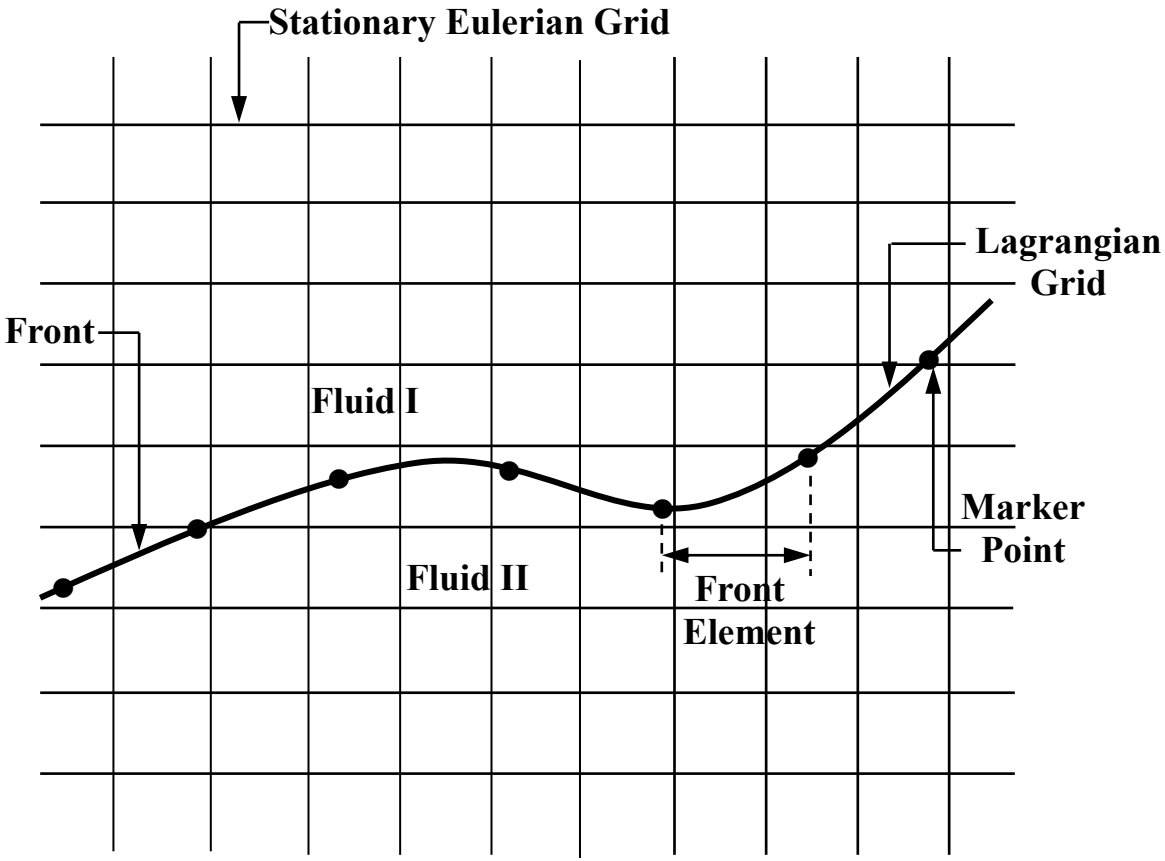

- Flow equations are solved on the Eulerian grid
- The Lagrangian grid used to track the interface and is dynamically restructured, i.e., small elements are deleted and large elements are split.

Unverdi & Tryggvason, JCP, (1992)
Tryggvason et al. JCP, (2001)

Thickness of interface ~ Mean free path (λ)

Extending to 3D

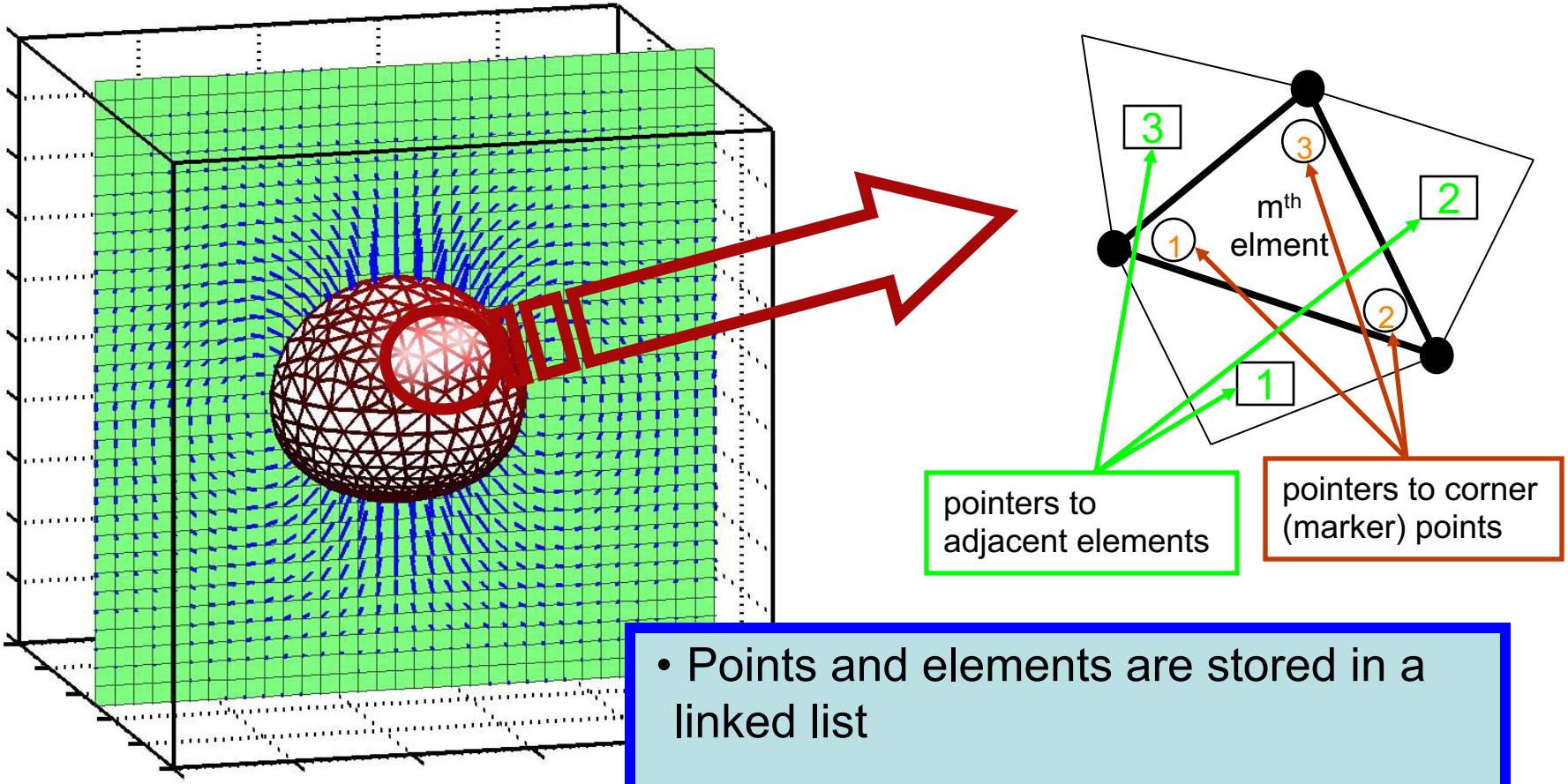

- Points and elements are stored in a linked list
- Only the coordinates are stored for the points
- The elements have pointers to the points and the adjacent elements

Tryggvason et al. *JCP*, (2001)

Validation: Buoyancy-Driven Rising Drops in a Constricted Channel

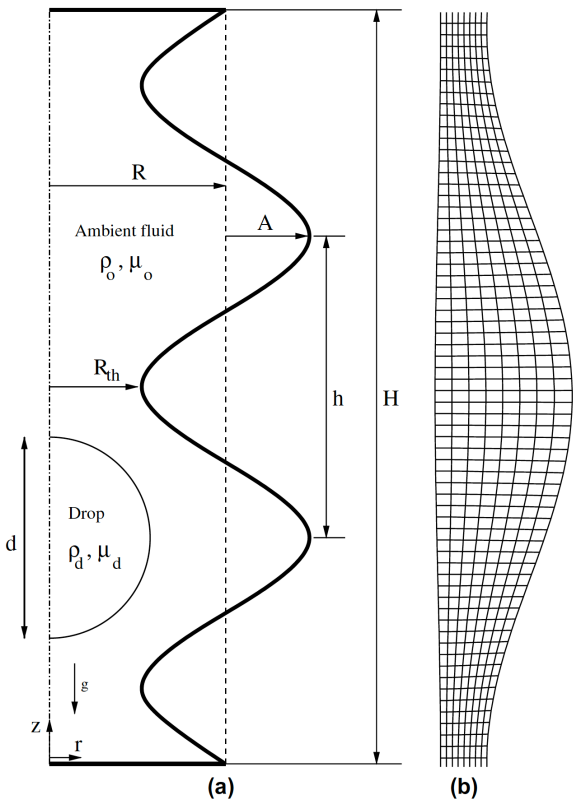

Computational setup and grid. (Olgac et al. 2006)

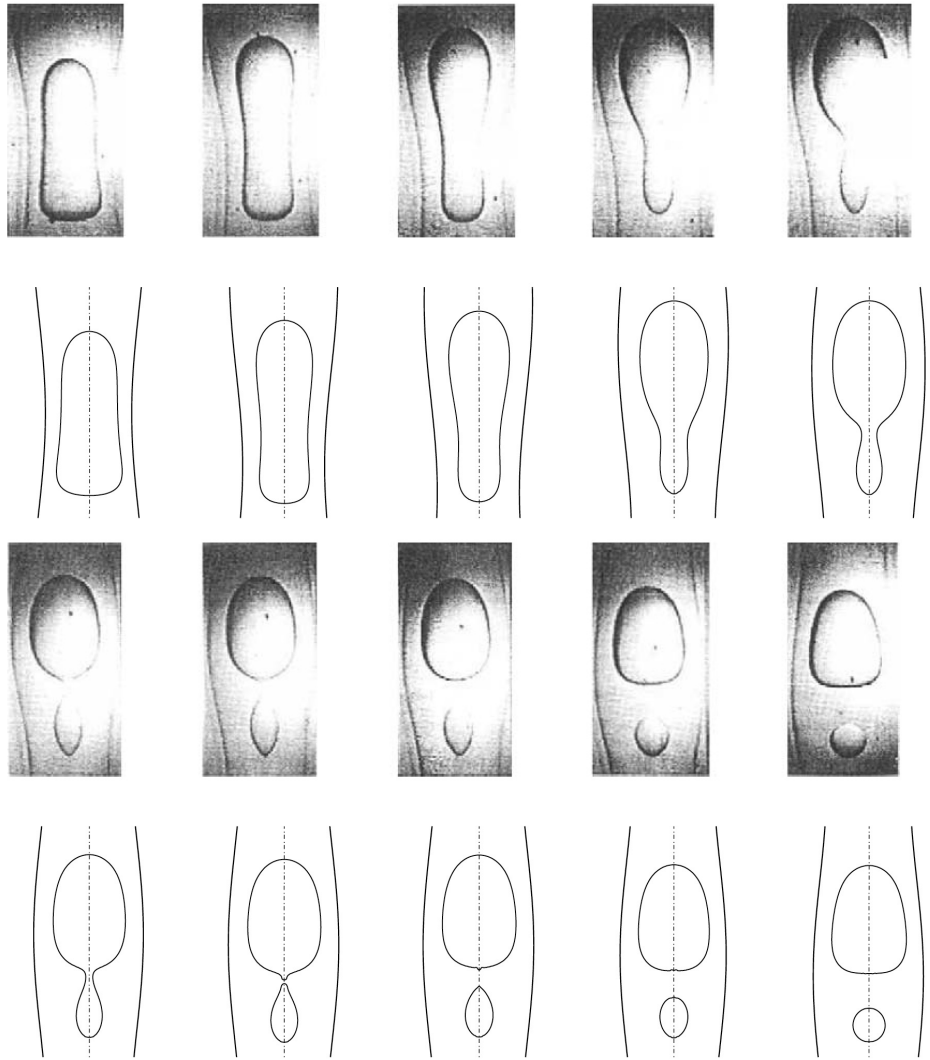

Hemmat & Borhan (1996) reported critical non-dimensional drop size as 0.85 which compares well with our value of 0.87

Power of Computations

Olgac et al. (2006)

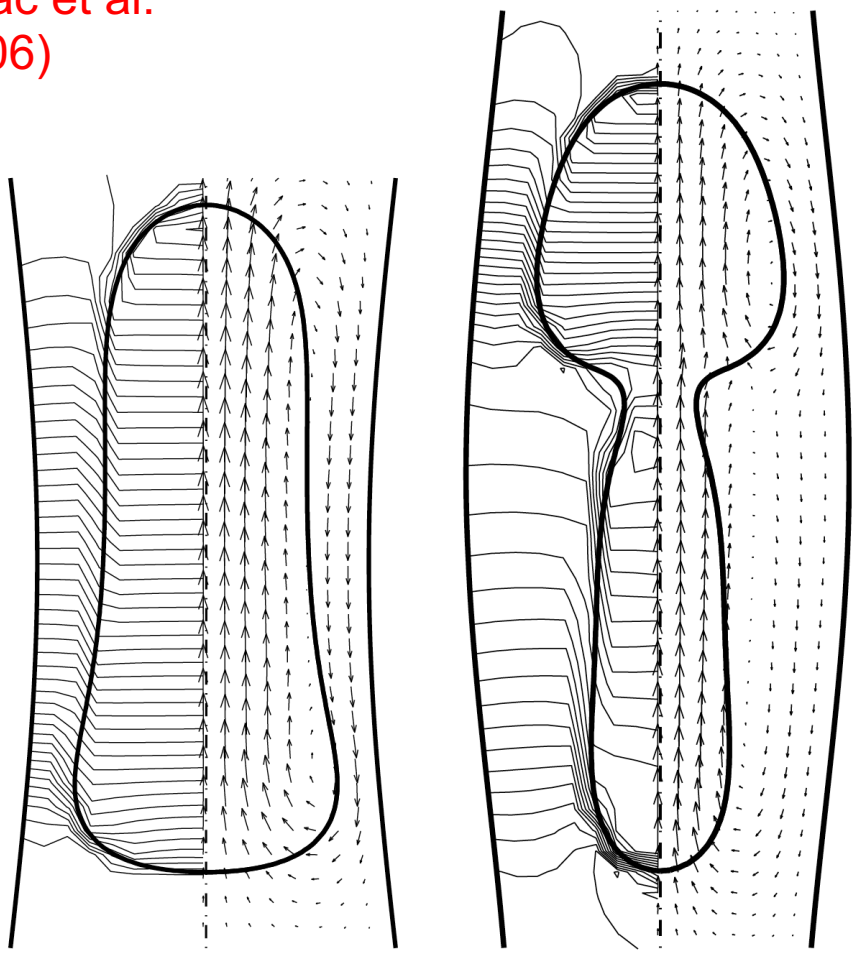

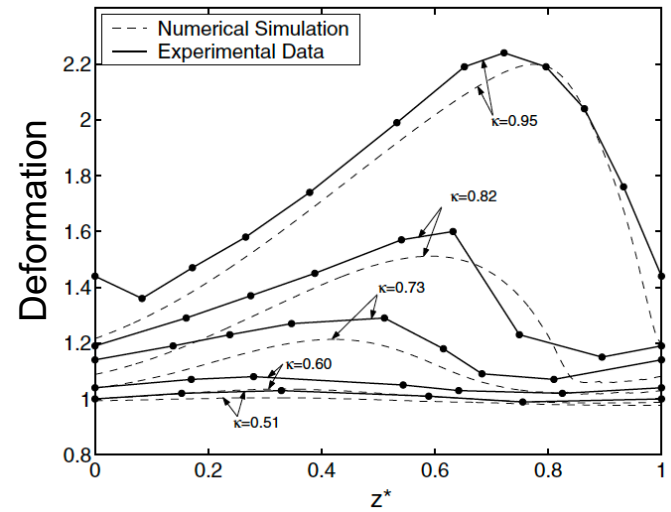

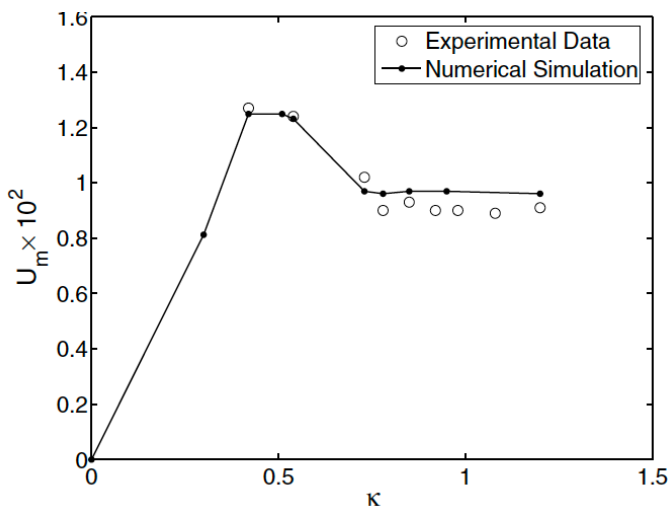

(Left)The drop shapes, the velocity field and pressure contours in the vicinity of the DEGG12, κ=0.92 drop. (Right) Comparison with the experimental data.

Phase Change

M. Irfan and **M. Muradoglu**, “A Front Tracking Method for Direct Numerical Simulation of Evaporation Process in A Multiphase System”, *Journal of Computational Physics,* **337:**132-153(2017)

M. Irfan and **M. Muradoglu**, “A front-tracking method for particle-resolved simulation of evaporation and combustion of a fuel droplet", *Computers&Fluids,* **174**:283-299 (2018)

Droplet Evaporation

Spray Combustion

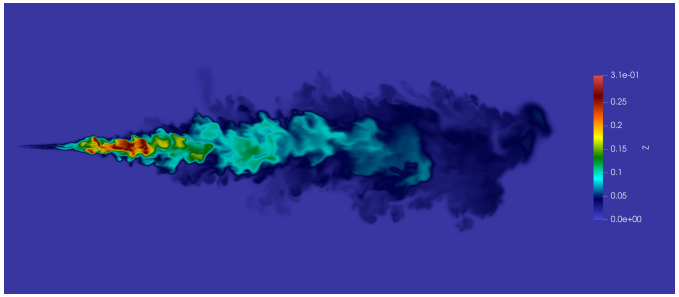

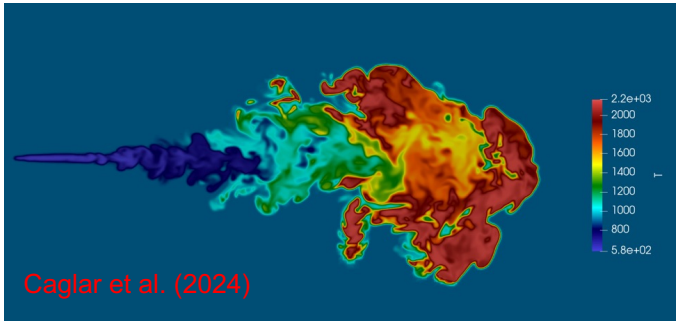

Caglar et al. (2024)

http://www.rocketlab.t.u-tokyo.ac.jp/member/inoue/chihilab_eng.html

Pattern Formation

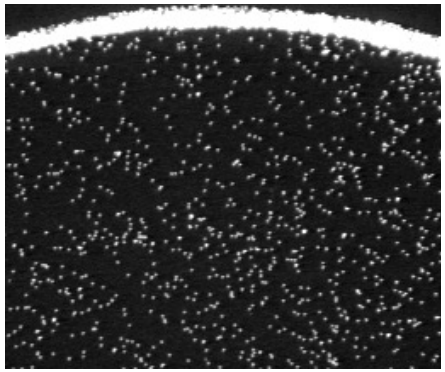

Coffee Ring Effect, Deegan et al., Nature (1997)

Governing Equations

Continuity Equation

$$\nabla \cdot \boldsymbol{u} = \frac{1}{h_{lg}}\left(\frac{1}{\rho_g} - \frac{1}{\rho_l}\right)\int_A \dot{q}\delta(\boldsymbol{x} - \boldsymbol{x}_f)dA$$

Momentum Equation

$$\frac{\partial \rho \boldsymbol{u}}{\partial t} + \nabla \cdot (\rho \boldsymbol{u}\boldsymbol{u}) = -\nabla p + \nabla \cdot \mu(\nabla \boldsymbol{u} + \nabla^T \boldsymbol{u}) + \boldsymbol{g}\Delta\rho + \int_A \sigma\kappa\boldsymbol{n}\delta(\boldsymbol{x} - \boldsymbol{x}_f)dA$$

Energy Equation

$$\frac{\partial \rho c_p T}{\partial t} + \nabla \cdot (\rho c_p \boldsymbol{u} T) = \nabla \cdot k\nabla T - \left[1 - (c_{pg} - c_{pl})\frac{T_{sat}}{h_{lg}}\right]\int_A \dot{q}\delta(\boldsymbol{x} - \boldsymbol{x}_f)dA$$

Species Mass Fraction

$$\frac{\partial \rho Y_\alpha}{\partial t} + \nabla \cdot (\rho \boldsymbol{u} Y_\alpha) = \nabla \cdot \rho D \nabla Y_\alpha + \dot{S}_\alpha(\boldsymbol{Y}, T), \qquad \alpha = 1,2,\ldots,n_s$$

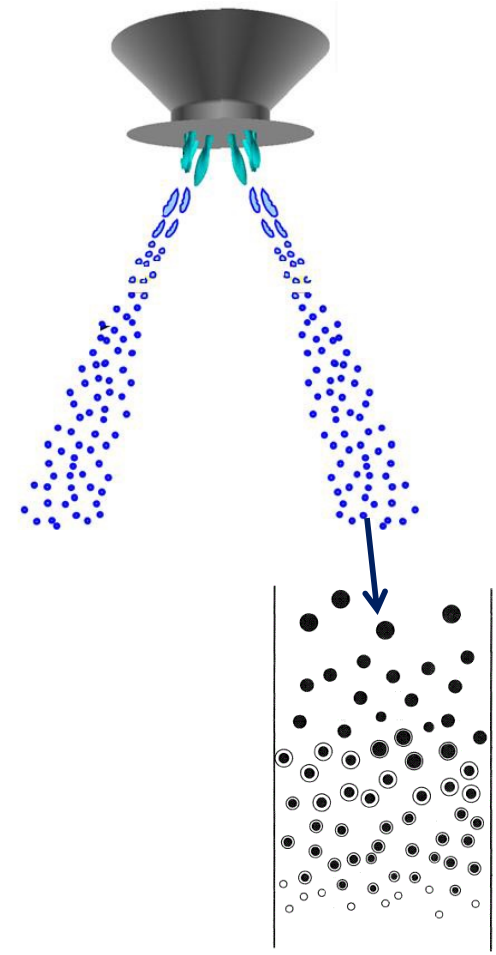

M. Irfan and M. Muradoglu, *JCP*, (2017)

Governing Equations

Continuity Equation

$$\nabla \cdot \boldsymbol{u} = \frac{1}{h_{lg}}\left(\frac{1}{\rho_g} - \frac{1}{\rho_l}\right)\int_A \dot{q}\delta(\boldsymbol{x} - \boldsymbol{x}_f)dA$$

Momentum Equation

$$\frac{\partial \boldsymbol{u}}{\partial t} + \nabla \cdot (\rho \boldsymbol{u}\boldsymbol{u}) = -\nabla p + \nabla \cdot \mu(\nabla \boldsymbol{u} + \nabla^T \boldsymbol{u}) + \boldsymbol{g}\Delta\rho + \int_A \left(\sigma(\Gamma)\kappa\boldsymbol{n} + \nabla_s \sigma(\Gamma)\right)\delta(\boldsymbol{x} - \boldsymbol{x}_f)dA$$

Energy Equation

$$\frac{\partial \rho c_p T}{\partial t} + \nabla \cdot (\rho c_p \boldsymbol{u} T) = \nabla \cdot k\nabla T - \left[1 - (c_{pg} - c_{pl})\frac{T_{sat}}{h_{lg}}\right]\int_A \dot{q}\delta(\boldsymbol{x} - \boldsymbol{x}_f)dA$$

Species Mass Fraction

$$\frac{\partial \rho Y_\alpha}{\partial t} + \nabla \cdot (\rho \boldsymbol{u} Y_\alpha) = \nabla \cdot \rho D \nabla Y_\alpha + \dot{S}_\alpha(\boldsymbol{Y}, T), \qquad \alpha = 1,2,\ldots,n_s$$

M. Irfan and M. Muradoglu, *JCP*, (2017)

Temperature Gradient Driven Phase Change

Continuity Equation:

$$\nabla \cdot \boldsymbol{u} = \frac{1}{h_{lg}}\left(\frac{1}{\rho_g} - \frac{1}{\rho_l}\right)\int_A \dot{q}\delta(\boldsymbol{x} - \boldsymbol{x}_f)dA$$

$$\dot{q} = k_g \left.\frac{\partial T}{\partial n}\right|_g - k_l \left.\frac{\partial T}{\partial n}\right|_l \approx \frac{1}{\eta h}\left[k_g(T_g - T_{sat}) - k_l\,(T_{sat} - T_l)\right]$$

$$T_g = T(x^+, y^+)$$
$$T_l = T(x^-, y^-)$$

$$\dot{q}_{i,j,k} = \sum_l \omega^l_{i,j,k}\dot{q}_{\Gamma_l}\frac{\Delta S_l}{h^3}$$

Energy Equation:

$$\frac{\partial \rho c T}{\partial t} + \nabla \cdot (\rho c T \boldsymbol{u}) = \nabla \cdot k \nabla T - \left[1 - (c_g - c_l)\frac{T_{sat}}{h_{lg}}\right]\int_A \dot{q}\delta(\boldsymbol{x} - \boldsymbol{x}_f)dA - \sum_\alpha \dot{\Omega}_\alpha h_\alpha(T)$$

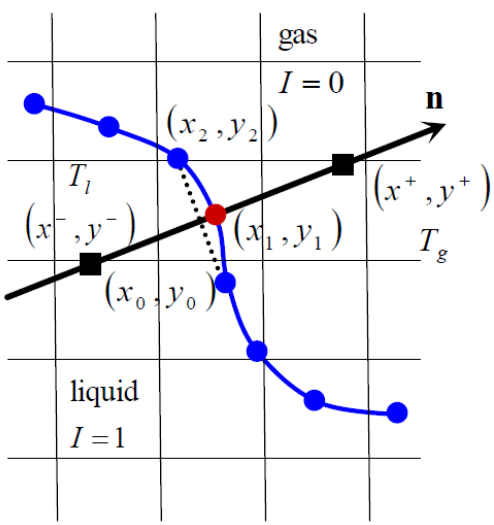

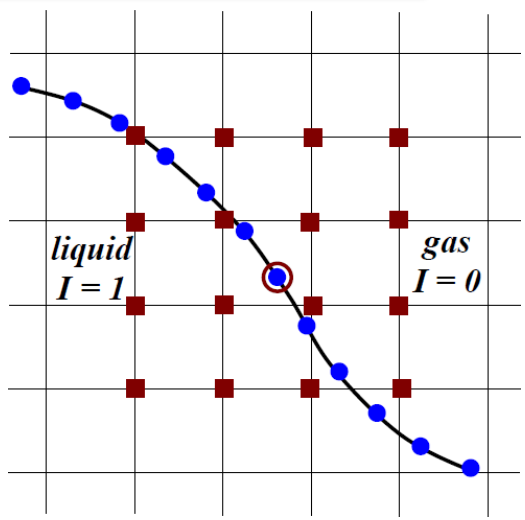

Indicator function

$$I(\mathrm{x}, \mathrm{t}) = \begin{cases} 1 & \text{in droplet phase,} \\ 0 & \text{in bulk phase.} \end{cases}$$

$$\phi = \phi_i I + \phi_o (1 - I)$$

$$\nabla^2 I = \nabla \cdot (\nabla I)$$

$$\nabla I = \int_A \vec{n}\,\delta(\vec{x} - \vec{x}_f)dA$$

Species Gradient Driven Phase Change

Species mass flux at interface

$$\frac{\partial \rho Y_\alpha}{\partial t} + \nabla \cdot (\rho \boldsymbol{u} Y_\alpha) = \nabla \cdot \rho D \nabla Y_\alpha + \boxed{\dot{S}_\alpha(\boldsymbol{Y}, T),} \qquad \alpha = 1,2,\ldots,n_s$$

$$\dot{S}_{\alpha_{i,j}} = \sum_l \omega_{i,j}^l \dot{m}_{\Gamma_l} \frac{\Delta S_l}{h^3}$$

$$\dot{m}_{\Gamma_l} = \frac{\rho_g D \nabla Y \cdot \boldsymbol{n}\big|_g^{\Gamma_l}}{1 - Y_{vap}^{\Gamma_l}}$$

Vapor concentration at interface

$$Y_{vap}^{\Gamma_l} = \frac{p_{vap}^{\Gamma_l} \mathcal{M}_{vap}}{(p_{atm} - p_{vap}^{\Gamma_l})\mathcal{M}_g + p_{vap}^{\Gamma_l} \mathcal{M}_{vap}}$$

$$p_{vap}^{\Gamma_l} = p_{atm} exp\left(-\frac{h_{lg}\mathcal{M}_{vap}}{\mathcal{R}}\left(\frac{1}{T^{\Gamma_l}} - \frac{1}{T^B}\right)\right)$$

Clausius-Clapeyron Relation

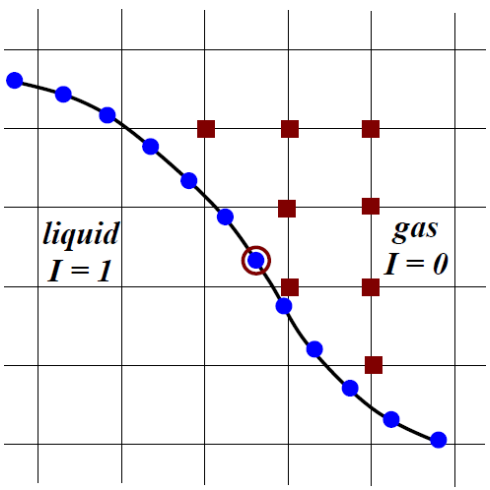

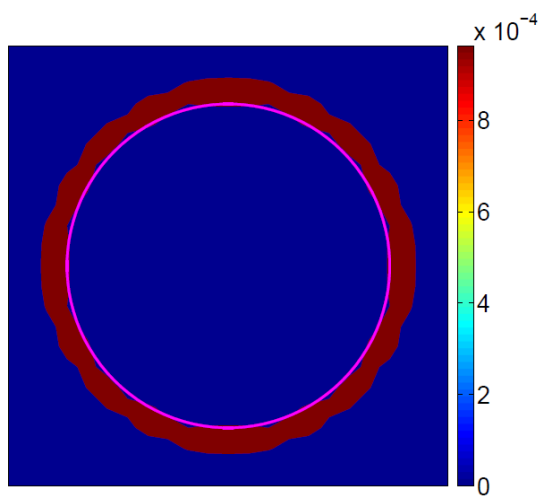

d^2-Law – Validation

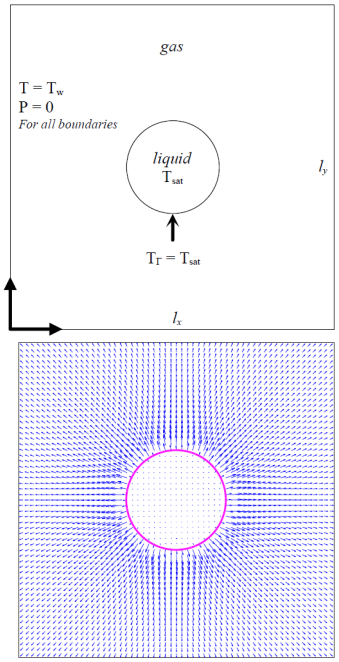

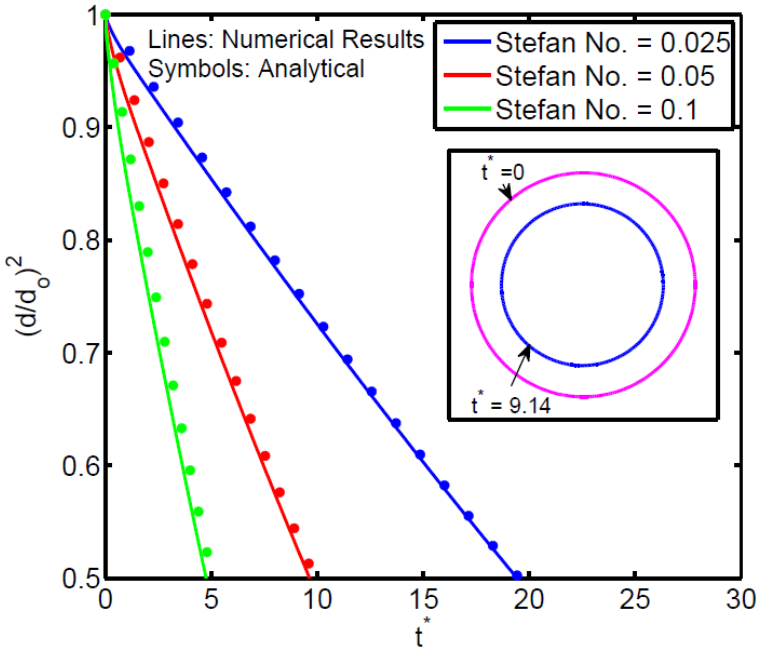

Analytical Solution:

$$\frac{dd^2}{dt} = -\frac{8\rho_g D_\alpha}{\rho_l}\frac{ln(1+B)}{ln(d_{ins}/d)}$$

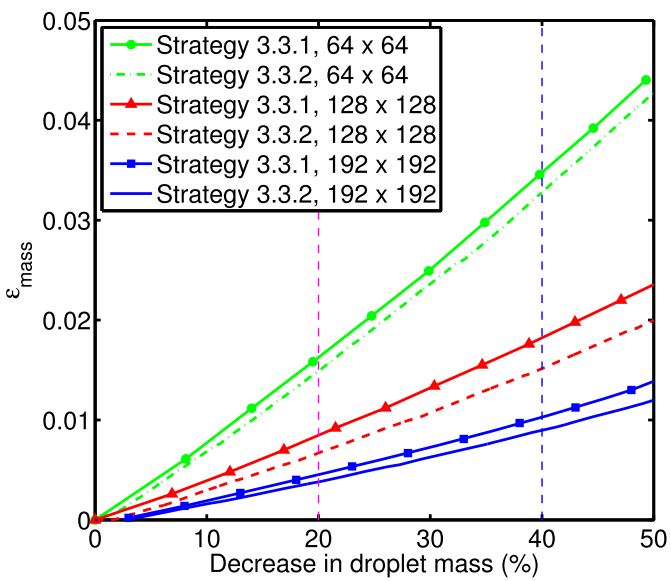

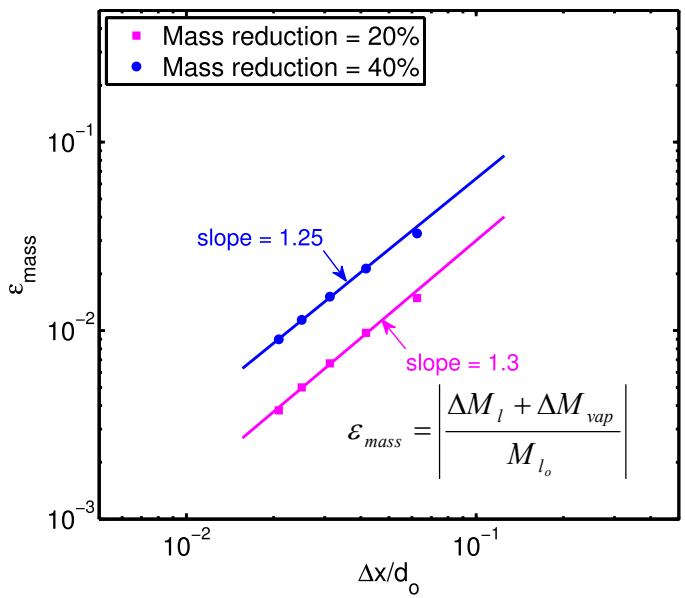

Close to only 1st order accuracy in space!

Moving Droplet – Grid Convergence

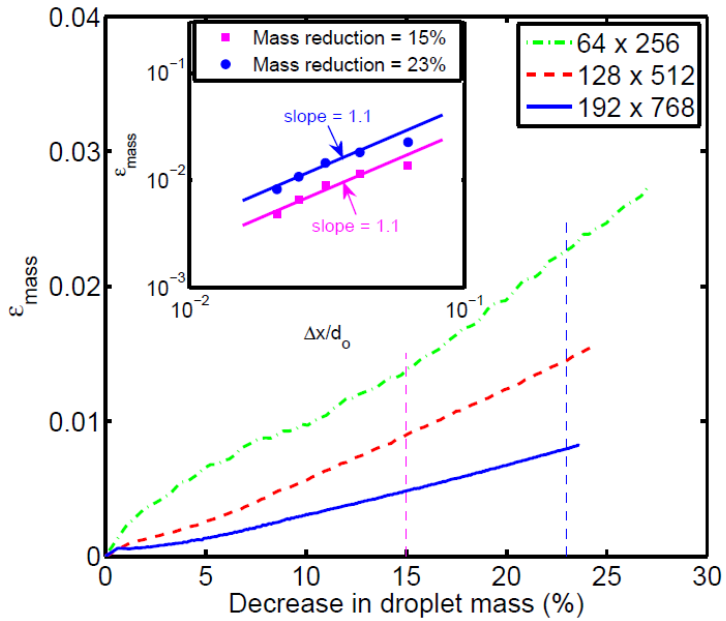

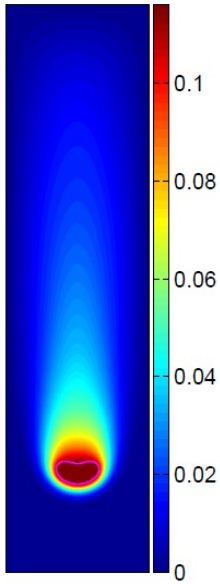

The droplet evaporates faster when it is more deformed

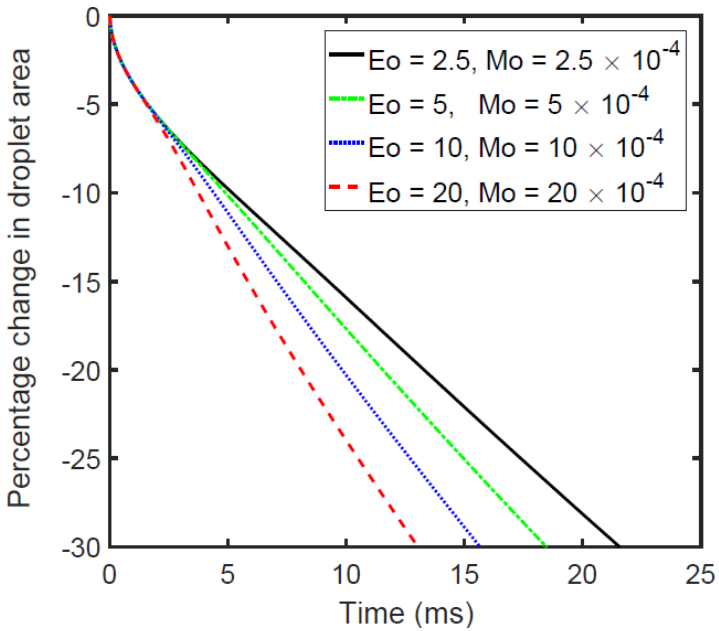

$$Eo = 10,\ Mo = 10 \times 10^{-4},\ St = 0.1,\ Sc = 1.0,$$
$$\gamma = 5,\ \zeta = 20,\ \text{Grid}: 128 \times 512$$

It is also only 1st order for this case!

Moving Droplet Evaporation: No Reaction

$$Eo = 10, M = 10^{-4}, Sc = 1, \gamma = 5, \zeta = 20, \text{Grid: } 192\times1536$$

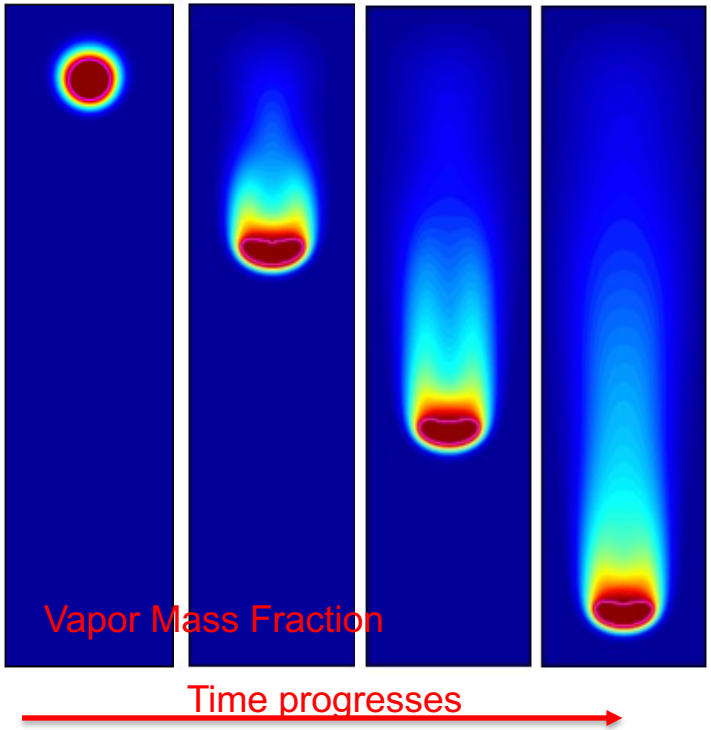

Single Droplet

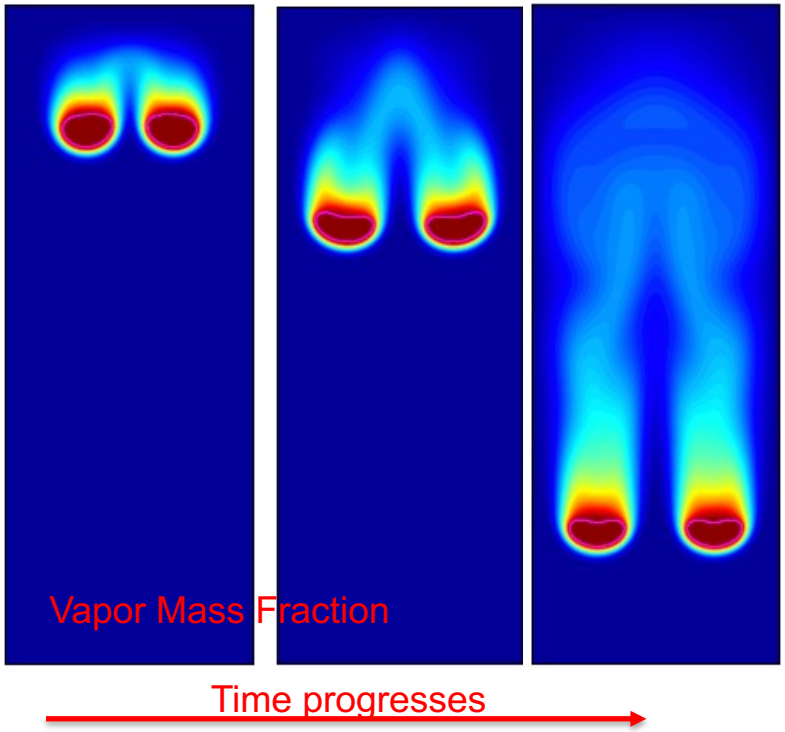

Two-Interacting Droplets

Chemical Reaction

Consider a single-step chemical mechanism for simplicity (generalization is straightforward)

$$F + aO_x \rightarrow bPr$$

Rate of fuel consumption is given by

$$\frac{d[X_F]}{dt} = -k_G(T)[X_F]^n \left[X_{O_x}\right]^m$$

$$k_G(T) = Aexp(-E_A/RT)$$

Reference: Turns S. An introduction to combustion: concepts and applications. New York: McGraw-Hill; 2000.

F = Fuel; O_x = Oxidizer; X = Mass fraction; k_G = Global rate coefficient; n, m = Reaction order; A = Pre − exponential factor; E_A = Activation energy; R = Universal gas constant

Example: A general Diesel fuel (e.g., n-heptane)

$$C_xH_y + a(O_2 + 3.76N_2) \rightarrow xCO_2 + (y/2)H_2O + 3.76aN_2$$

$$a = x + y/4$$

ODE Solver: Chemkin-II (Kee R., Rupley F., Miller J.. Chemkin-II: A fortran chemical kinetics package for the analysis of gas-phase chemical kinetics. 1989.)

Chemical Kinetics: CHEMKIN

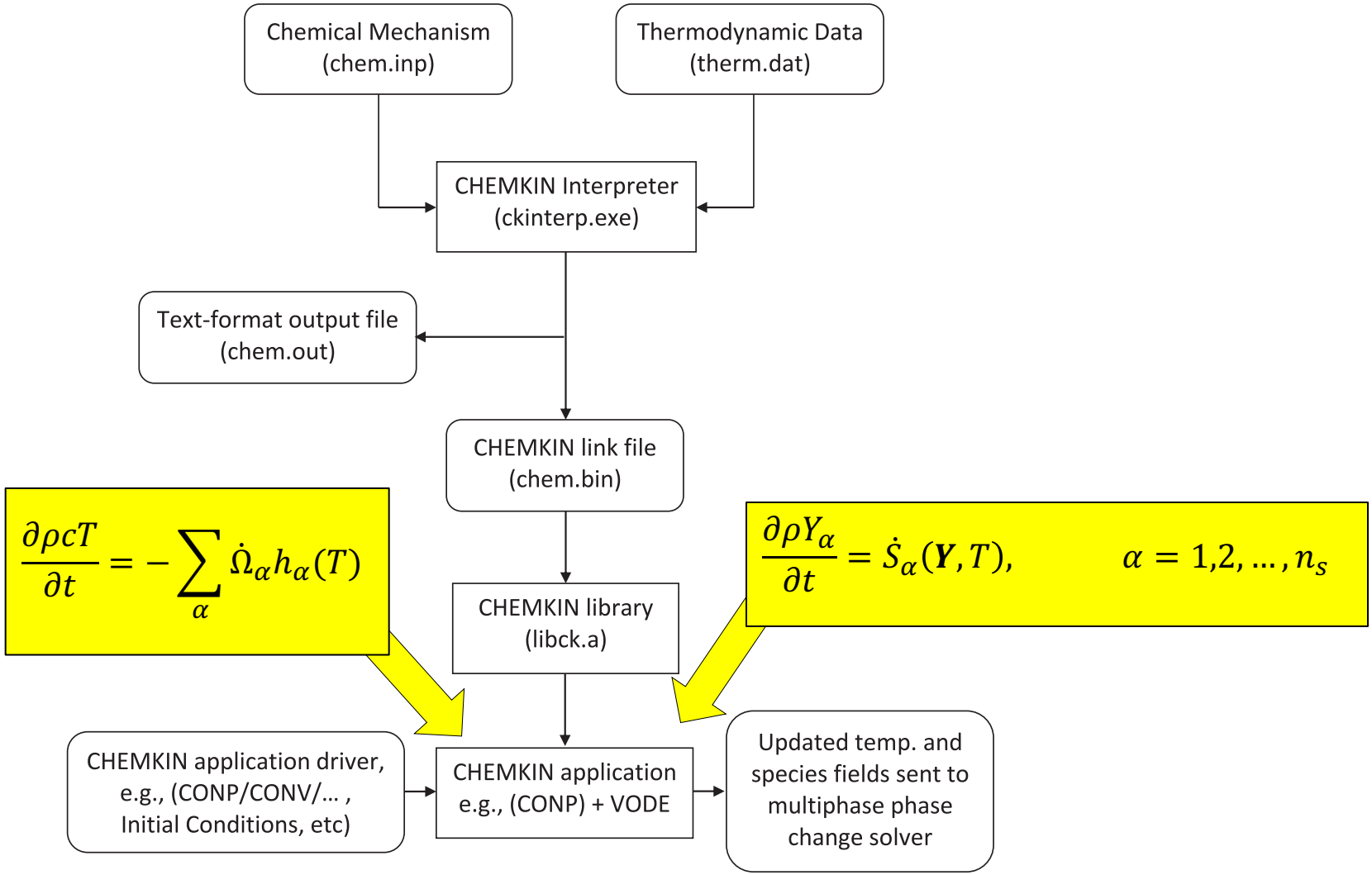

n-Heptane Droplet Combustion

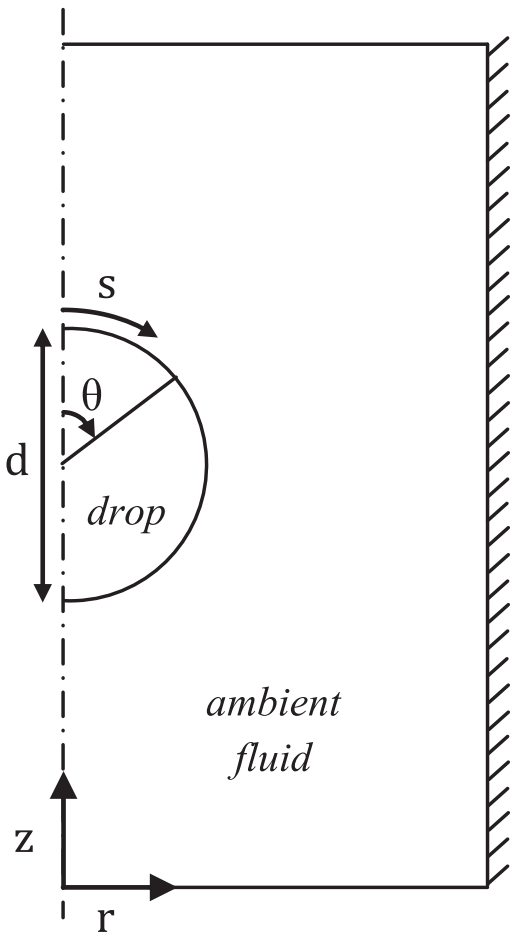

A single-step n-heptane-air chemistry:

$C_7H_{16} + 11O_2 \rightarrow 7CO_2 + 8H_2O$

$T_d = 371.6K, T_g = 500K$

Domain: $5d_0 \times 10d_0$

Ambient Air: 79% N_2 & 21%O_2

Ignition: By temperature heat source

n-Heptane Droplet Combustion: Stationary Case

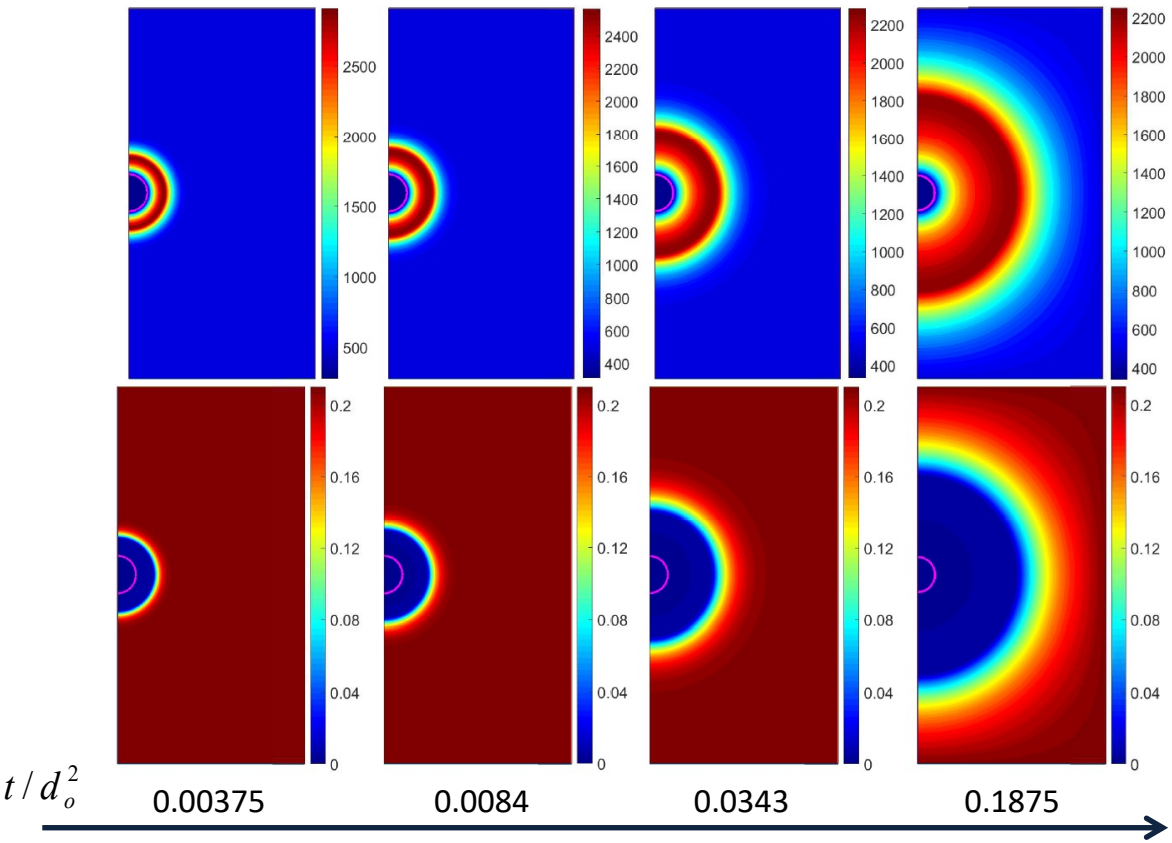

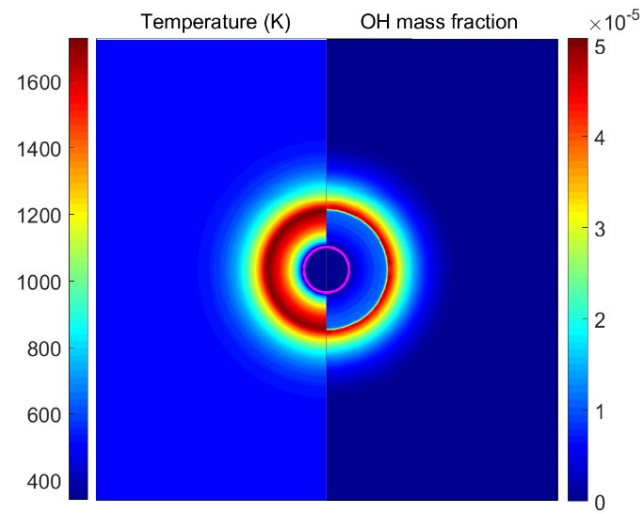

$T_{d,o} = 371.6\text{K},\ T_g = 500\text{K},\ p = 10\ \text{atm}$

Domain : $(5d_o, 10d_o)$ where $d_o = 0.4\text{mm}$

Ambient Air : 79% N_2 & 21% O_2 (by vol.)

Ignition : By temporary heat source

Reduced Chemistry : 25 Species & 26 Reactions (Maroteaux and Neol)

Moving and Burning Droplet

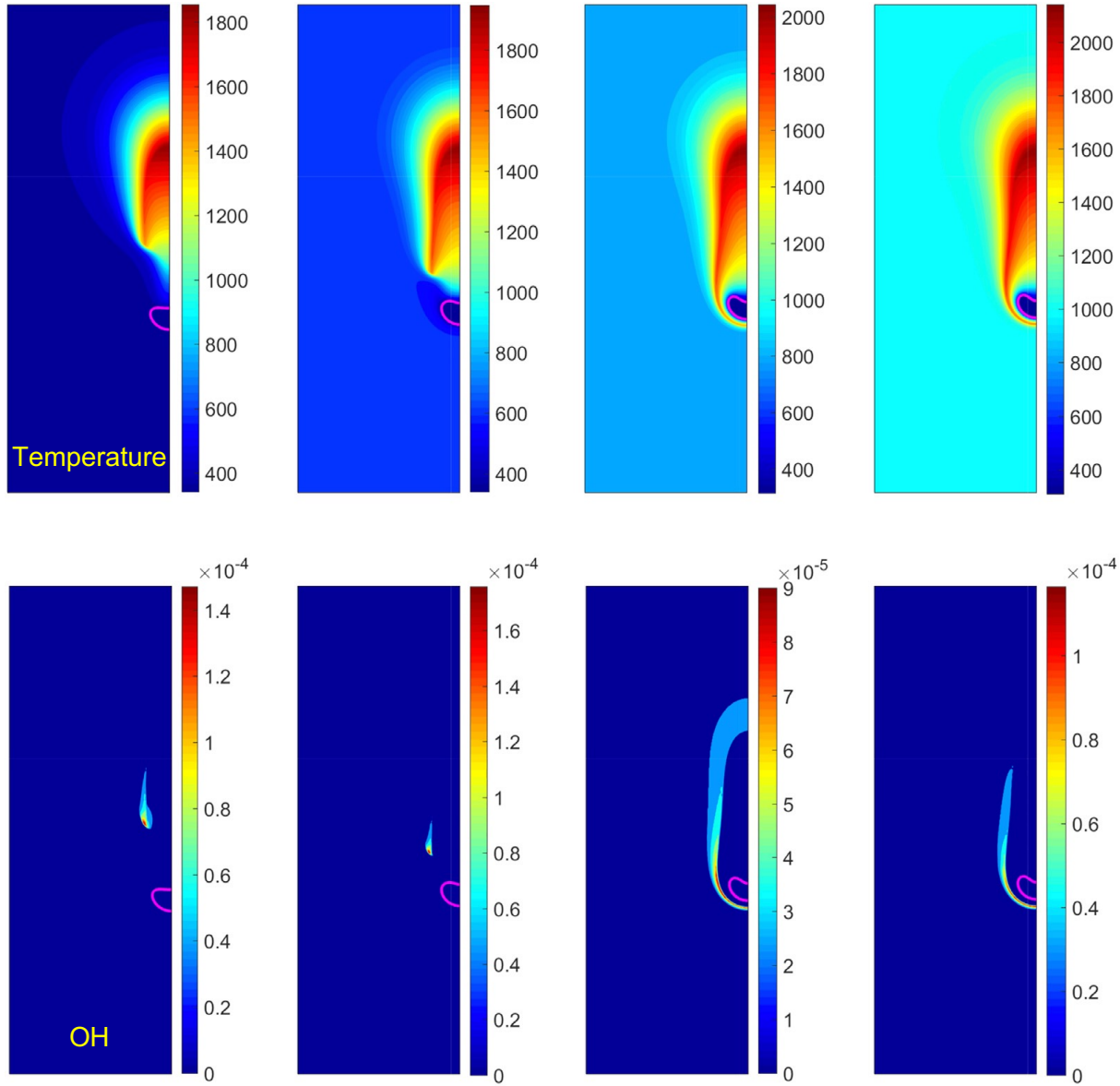

(a) $T_g = 400$ K (b) $T_g = 600$ K (c) $T_g = 800$ K (d) $T_g = 1000$ K

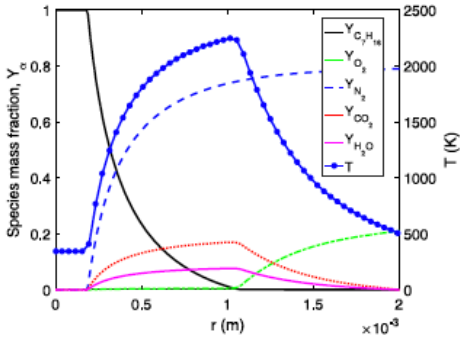

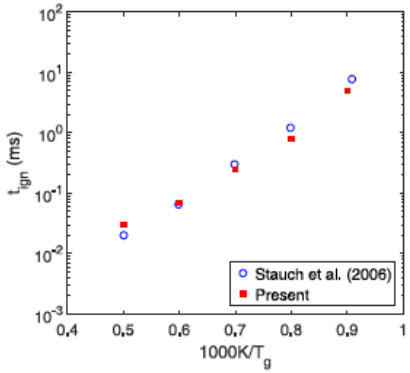

T_g = Ambient temperature

Hybrid Front-Tracking/Immersed-Boundary Method

- **Motivation:**
  - Distributing source term results in only 1st order accuracy in space
  - Extreme grid resolution is required to resolve thin mass boundary layer especially at high Peclet numbers
  - Thus, a second order method is highly desirable
- **Approach:**
  - Combine the front-tracking method with a sharp-interface immersed boundary (IBM) method of Mittal et al. (2008)
  - Also use this methodology to treat mass/heat transfer from solid particles immersed in fluid

F. Salimnezhad, H. Turkeri, I. Gokalp and **M. Muradoglu**, “A hybrid immersed-boundary/front-tracking method for interface-resolved simulation of droplet evaporation", *Computers & Fluids,* **291** (2025)

Sharp-Interface Immersed-Boundary Method

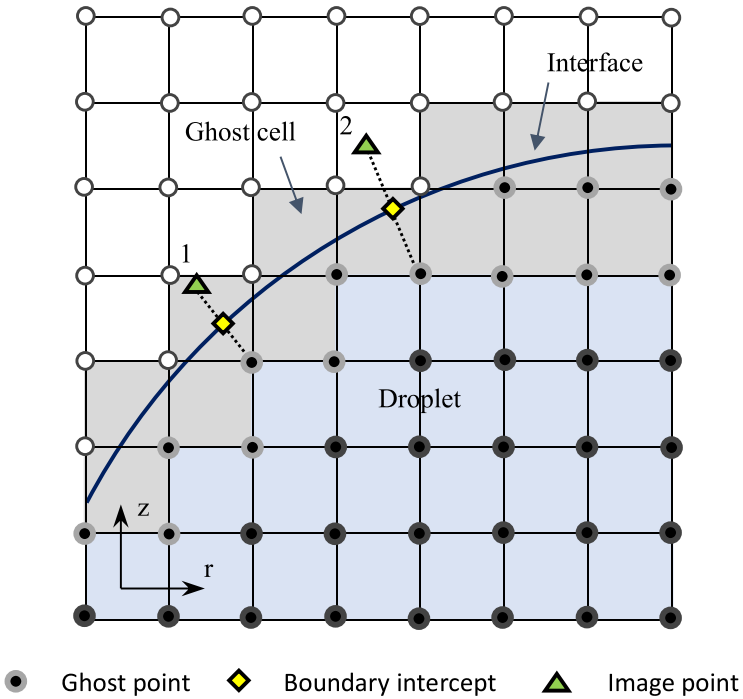

The dispersed phase could be fluid or solid or both!

Following Mittal et al. (2008)

- The cells cut by the interface are identified
- The mass-fraction field is represented by a bi-linear (tri-linear in 3D) function

$$Y(r,z) = a_1 rz + a_2 r + a_3 z + a_4.$$

- A vandermonde system is formed and solved to determine values in the ghost cells such that the boundary conditions are satisfied

$$[V]\{A\} = \{Y\}$$

$$[V] = \begin{bmatrix} r_1 z_1 & r_1 & z_1 & 1 \\ r_2 z_2 & r_2 & z_2 & 1 \\ r_3 z_3 & r_3 & z_3 & 1 \\ r_4 z_4 & r_4 & z_4 & 1 \end{bmatrix}; \ \{A\} = \begin{Bmatrix} a_1 \\ a_2 \\ a_3 \\ a_4 \end{Bmatrix}; \ \{Y\} = \begin{Bmatrix} Y_1 \\ Y_2 \\ Y_3 \\ Y_4 \end{Bmatrix}.$$

Validation-Falling droplet under gravity

Eo = 24

Eo = 48

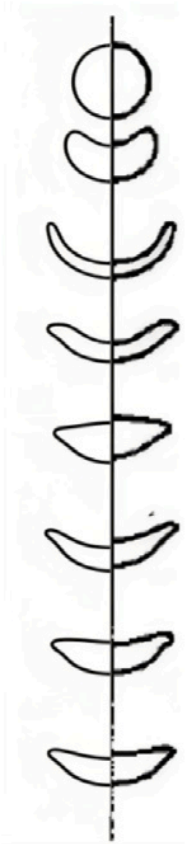

No phase change

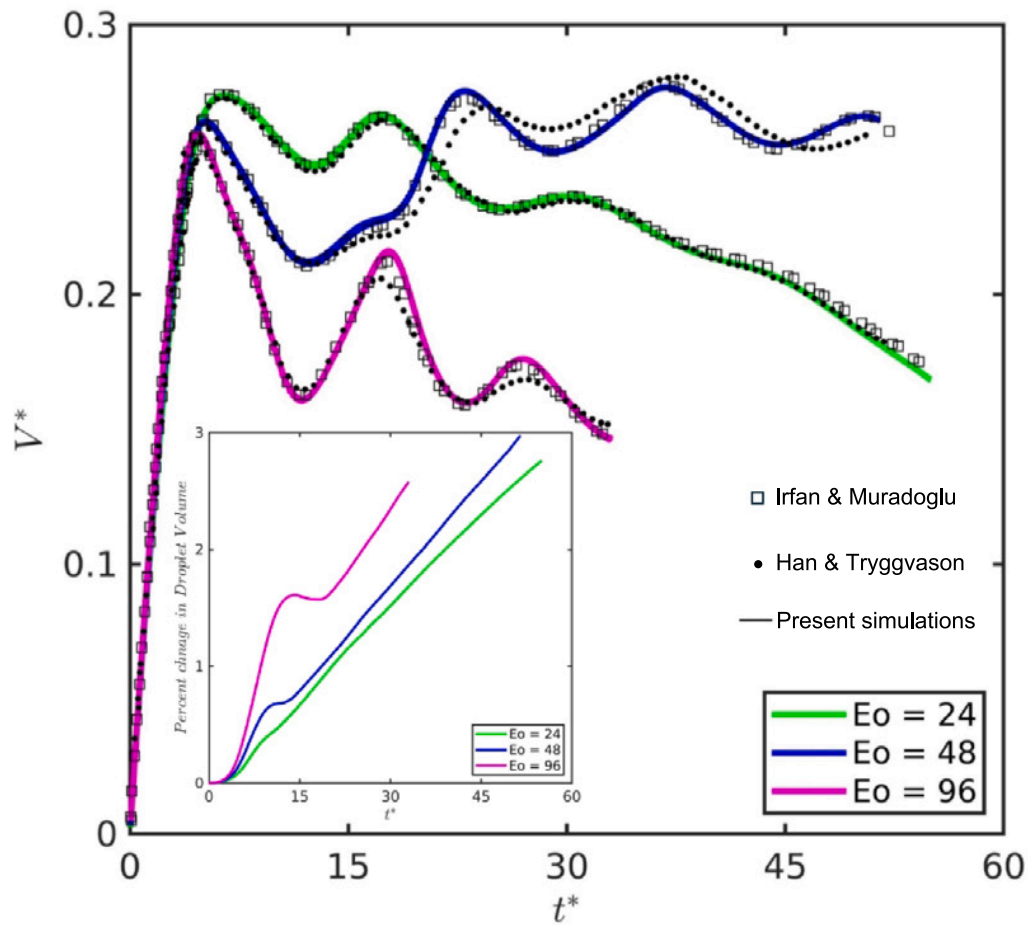

Validation-Mass transfer from a solid sphere

Flow is from bottom to upward

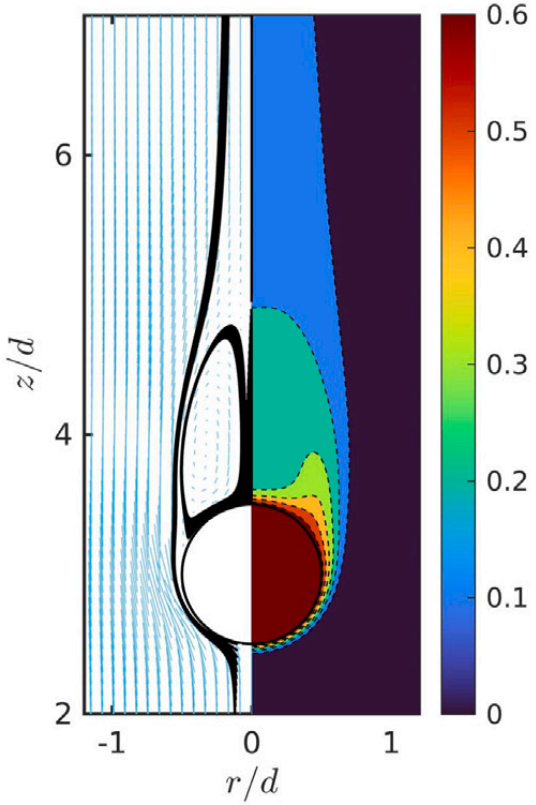

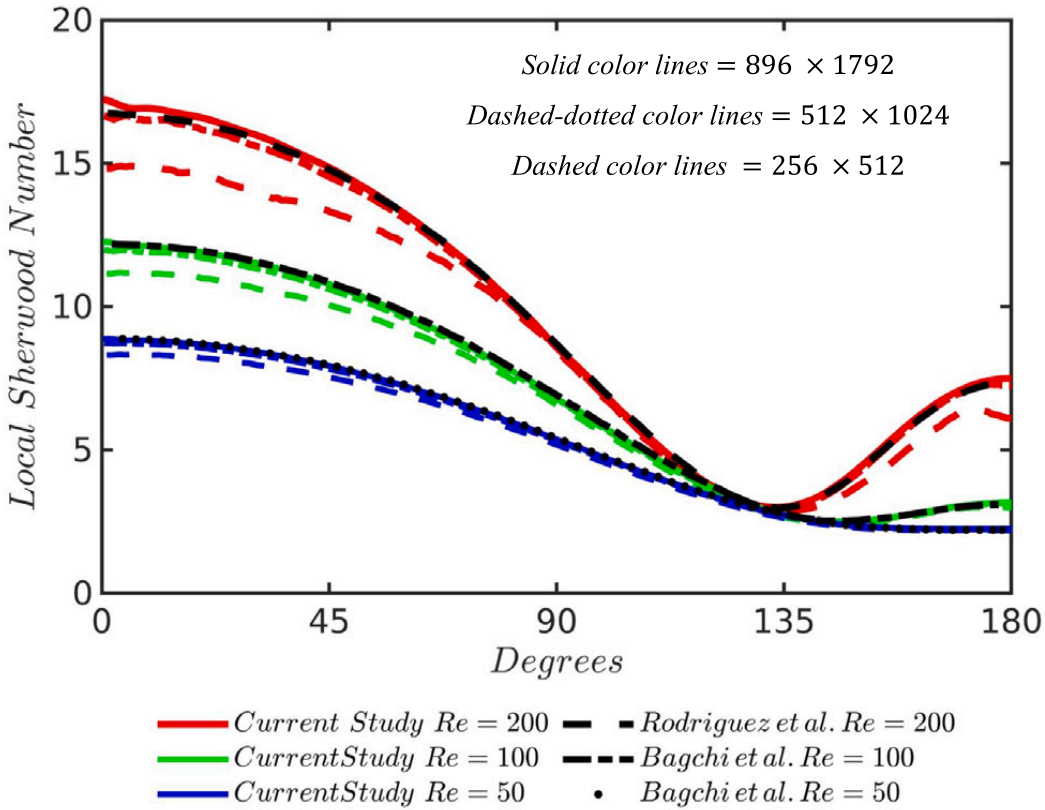

Left: flow velocity & streamlines
Right: mass fraction

Validation: d^2 – law

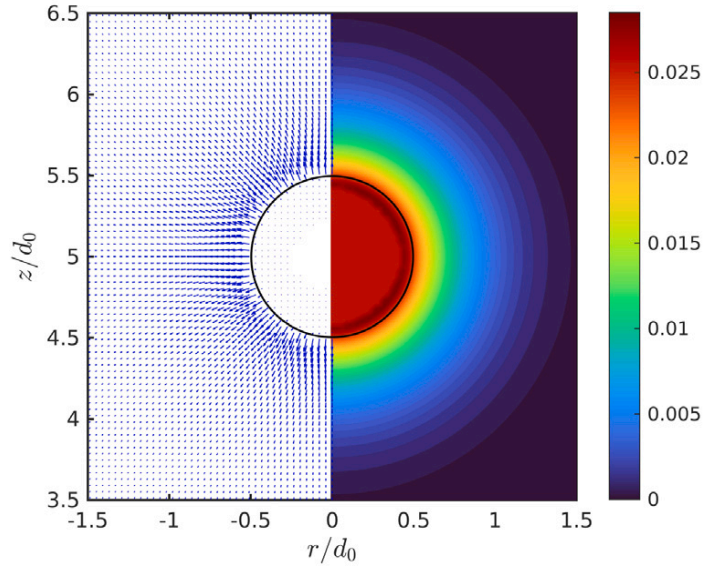

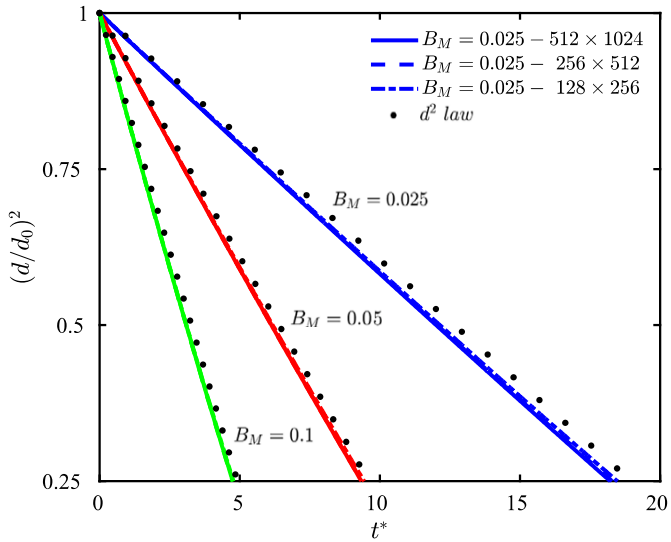

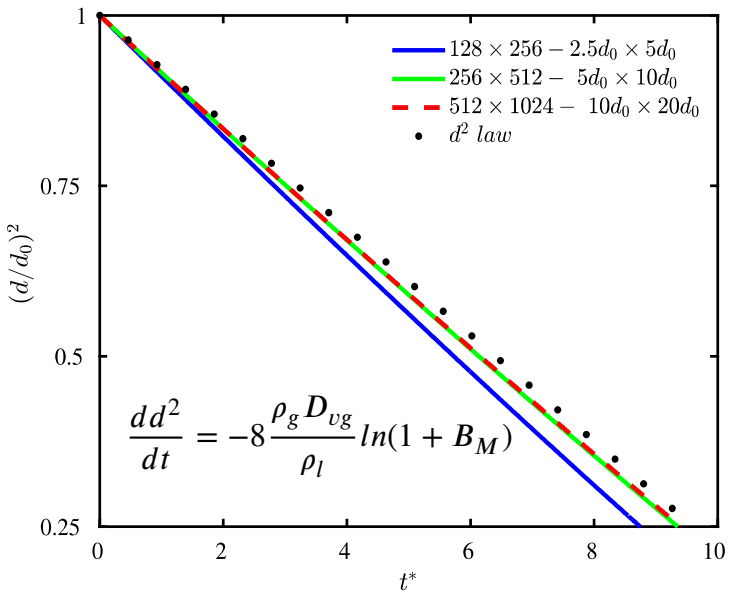

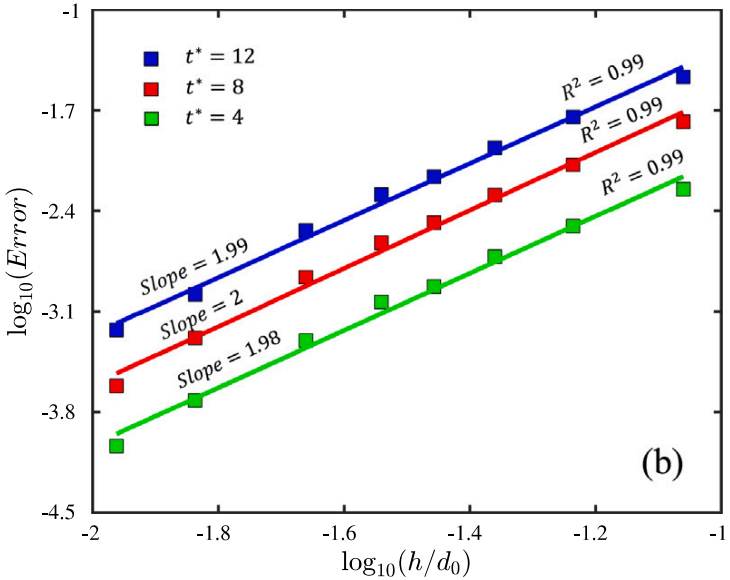

Second order accurate in space!

Validation: Wet-bulb temperature

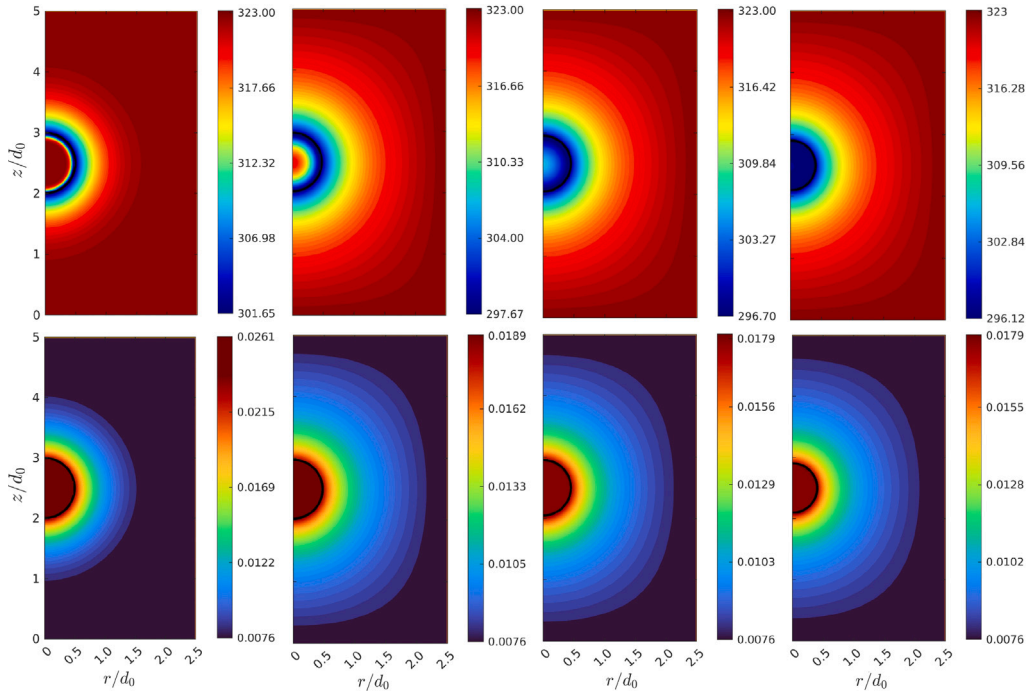

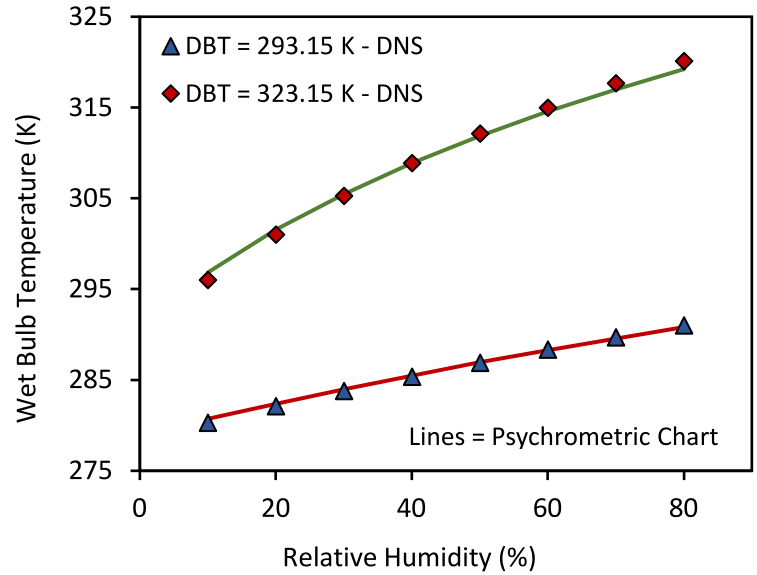

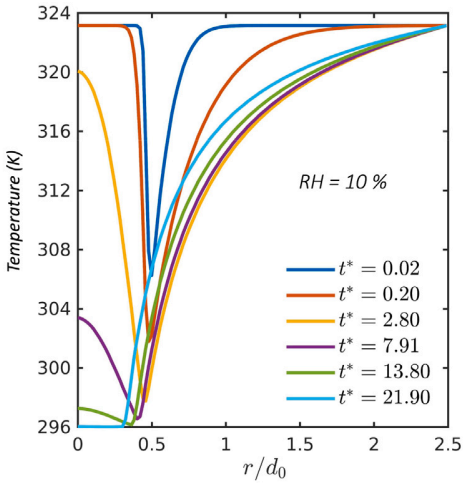

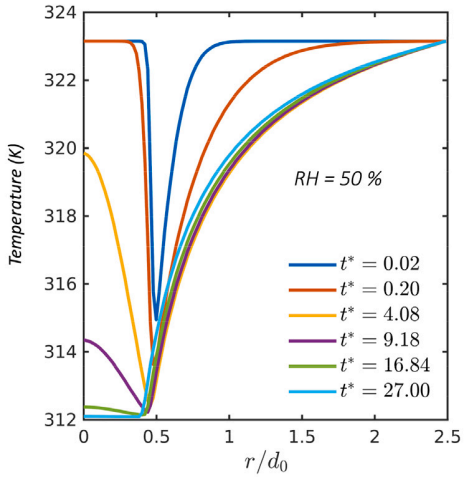

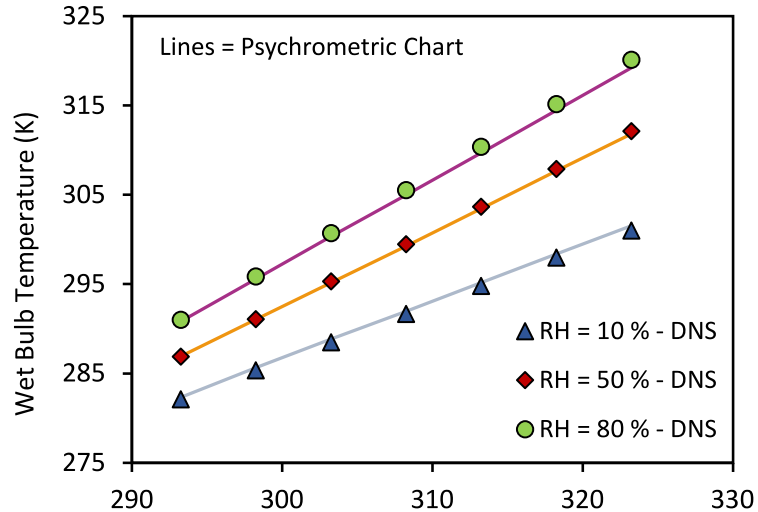

Droplet evaporation under convection

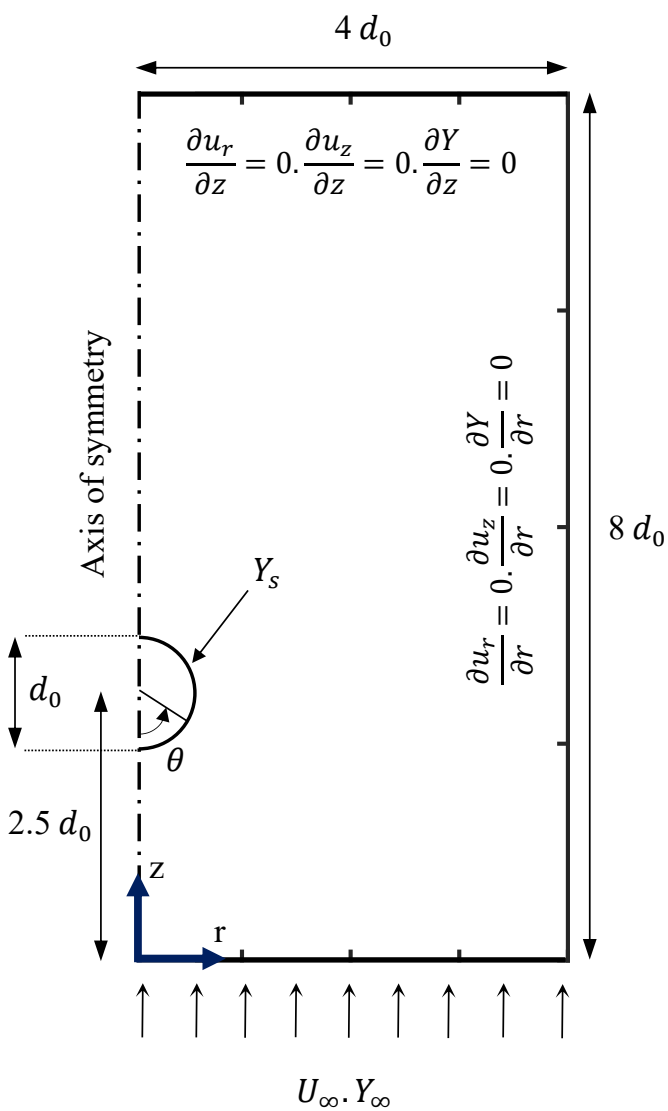

- Following Rusche. (2003), moving reference frame (MRF) is used to keep droplet fixed in computational domain:

$$\rho \frac{\partial \boldsymbol{u}_{rel}}{\partial t} + \rho \left[\nabla \cdot (\boldsymbol{u}_{rel}\boldsymbol{u}_{rel}) - \boldsymbol{u}_{rel} (\nabla \cdot \boldsymbol{u}_{rel})\right] = -\nabla p + \rho (\boldsymbol{a}_{MRF})$$
$$+\nabla \cdot \mu \left(\nabla \boldsymbol{u}_{rel} + \nabla \boldsymbol{u}_{rel}^T\right) + \int_A \sigma \kappa \boldsymbol{n} \delta (\boldsymbol{x} - \boldsymbol{x}_\Gamma)\, dA,$$

where

$\boldsymbol{a}_{MRF}$ = acceleration computed at every time step
$\boldsymbol{u}_{rel}$ = relative velocity

- The relevant flow parameters:

$$Re = \frac{\rho_g U_\infty d_0}{\mu_g}, \quad We = \frac{\rho_g {U_\infty}^2 d_0}{\sigma}, \quad Sc = \frac{\mu_g}{\rho_g D_{vg}},$$
$$Sh = \frac{-d_0}{Y_\Gamma - Y_\infty}\left(\frac{\partial Y}{\partial n}\right), \quad B_M = \frac{Y_\Gamma - Y_\infty}{1 - Y_\Gamma}.$$

- Simulations are performed for

$0 < Re \leq 200, \qquad 0 \leq We \leq 9, \qquad \leq B_M \leq 15$

Low-order models

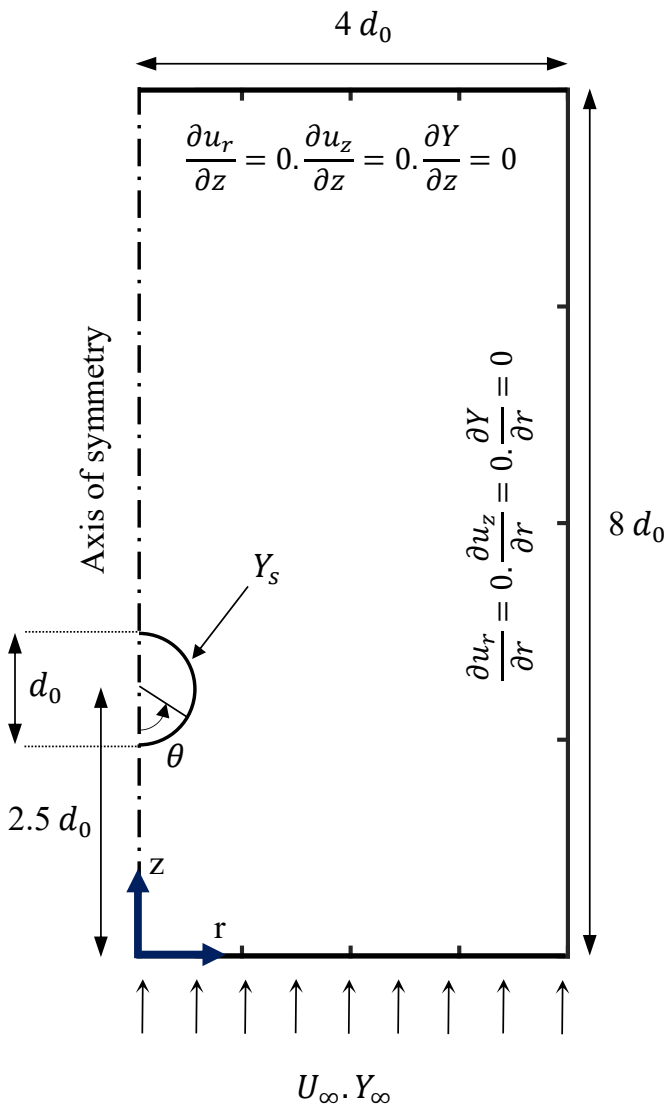

- The *classical* model (Spalding 1953, Sazhin 2017):

$$Sh = Sh_0 \frac{\ln(1 + B_M)}{B_M}$$

where Sh_0 is usually obtained from *Ranz-Marshall* correlation (Ranz 1952)

$$Sh_0 = 2 + 0.552 Re^{1/2} Sc^{1/3}$$

- The *Abramzon-Sirignano* model (Abramzon & Sirignano 1989):

$$Sh = \left(2 + \frac{Sh_0 - 2}{F_M}\right) \frac{\ln(1 + B_M)}{B_M}$$

$$F_M = (1 + B_M)^{0.7} \frac{\ln(1 + B_M)}{B_M}$$

where the droplet is approximated to be collection of wedges and the *Falkner–Skan* boundary layer solution is used (*Sirignano 2010)*.

The correction factor, F_M, accounts for BL thickening due to Stefan flow

Grid Convergence

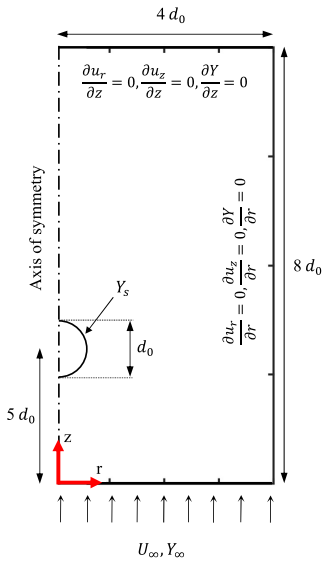

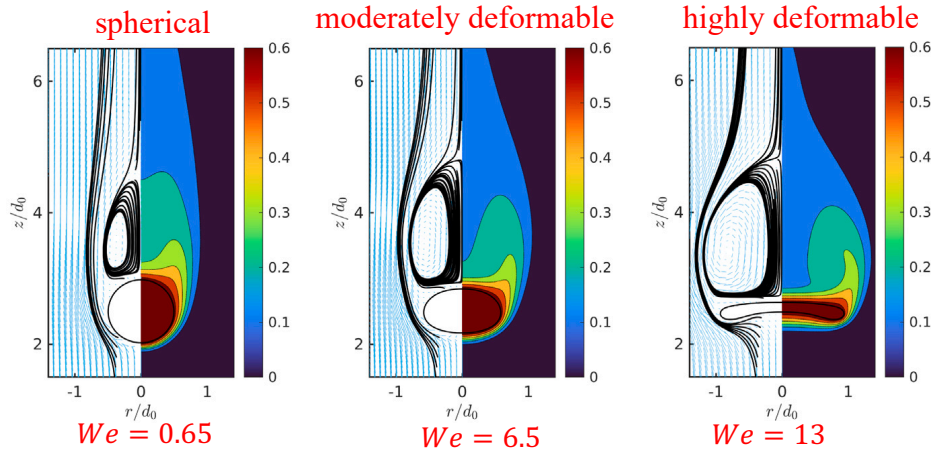

$$\frac{\rho_l}{\rho_g} = 25.75$$
$$\frac{\mu_l}{\mu_g} = 15.34$$
$$B_M = 2$$
$$Sc = 0.7$$
$$Re = 100$$

Domain: $4d_0 \times 8d_0$

Grid: 512×1024

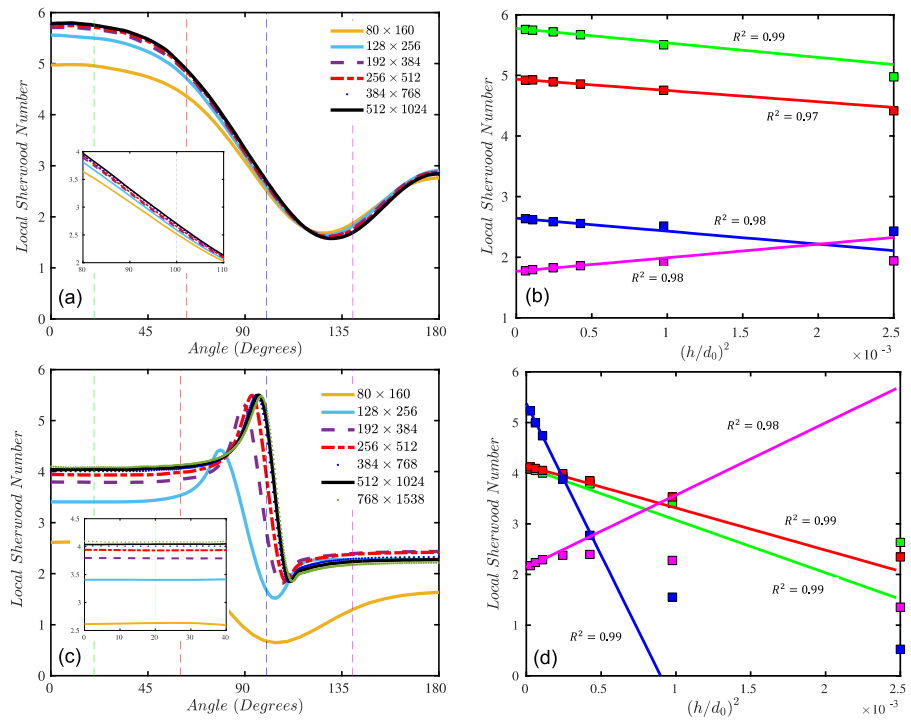

Second order accurate in space!

Effects of Stefan Flow

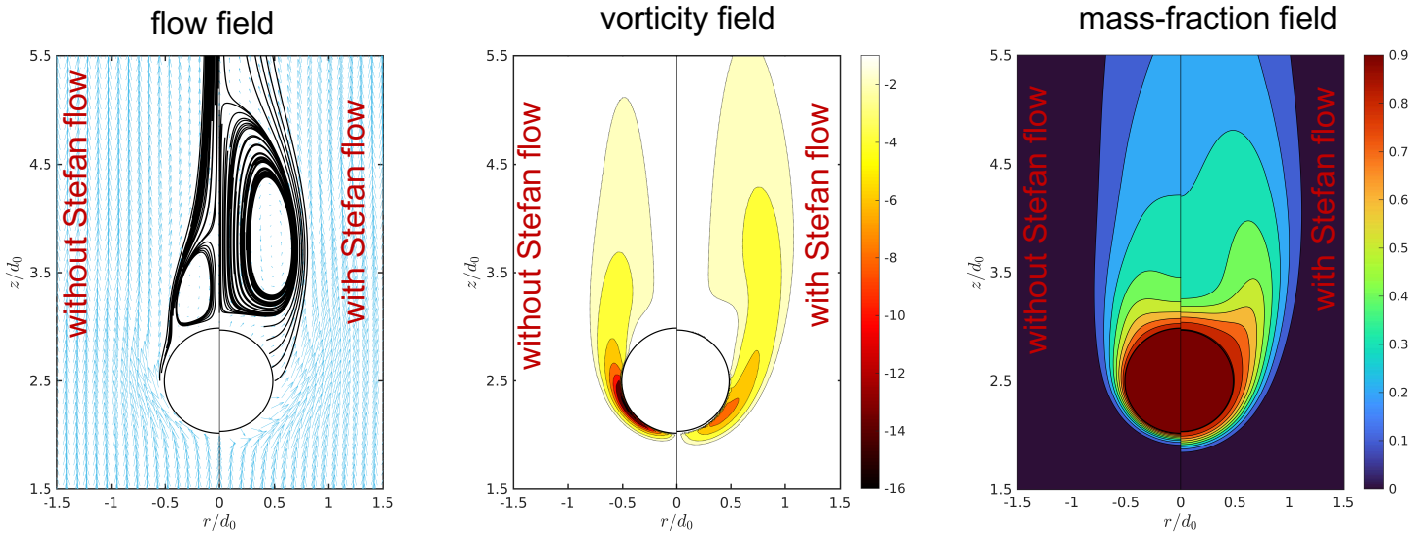

$$Re = 100, We = 0.65, B_M = 10, t^* = 10.$$

Stefan flow

- thickens the boundary layer
- promotes early flow separation
- enlarges the recirculation zone

Effects of Reynolds Number

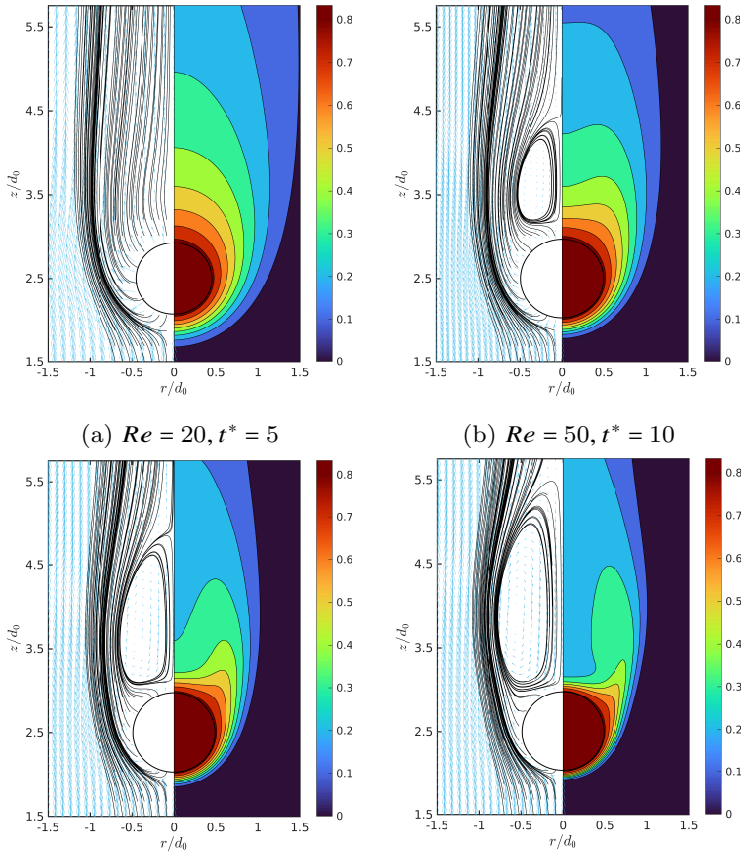

(a) $Re = 20, t^* = 5$ (b) $Re = 50, t^* = 10$

(c) $Re = 100, t^* = 20$ (d) $Re = 200, t^* = 30$

$$We = 0.65, B_M = 5$$

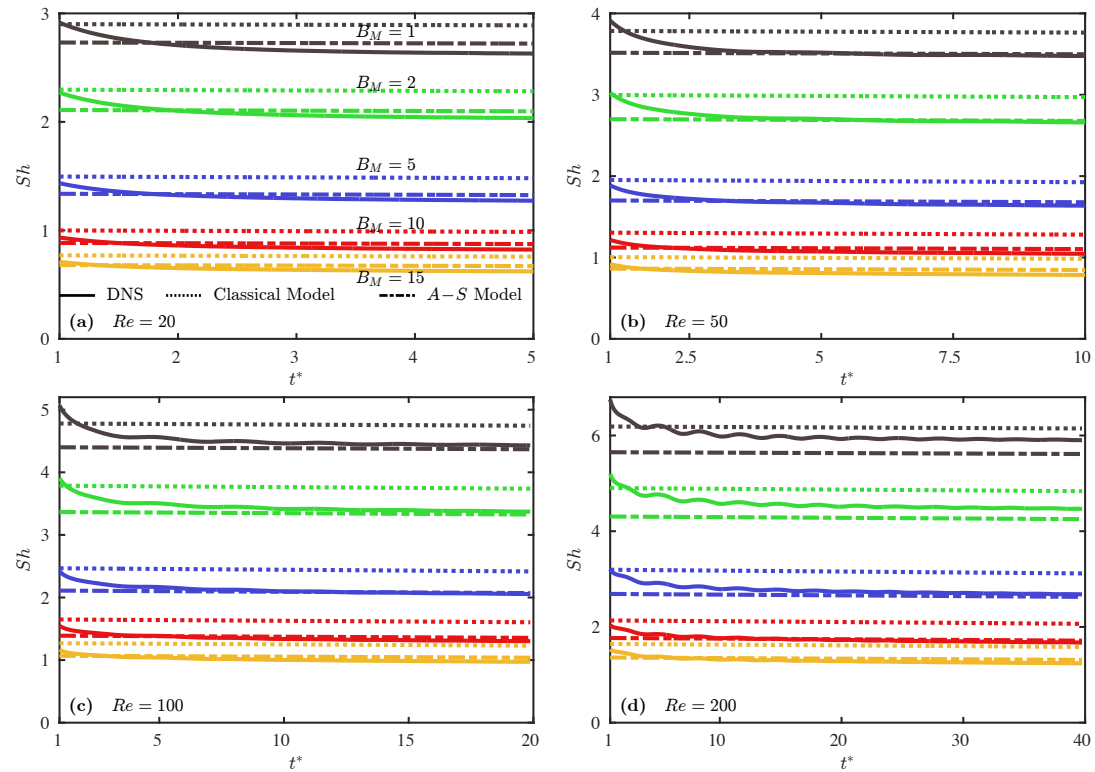

- The classical model overpredicts evaporation rate
- The Abramzon-Sirignano model outperforms the classical model

Effects of Reynolds Number

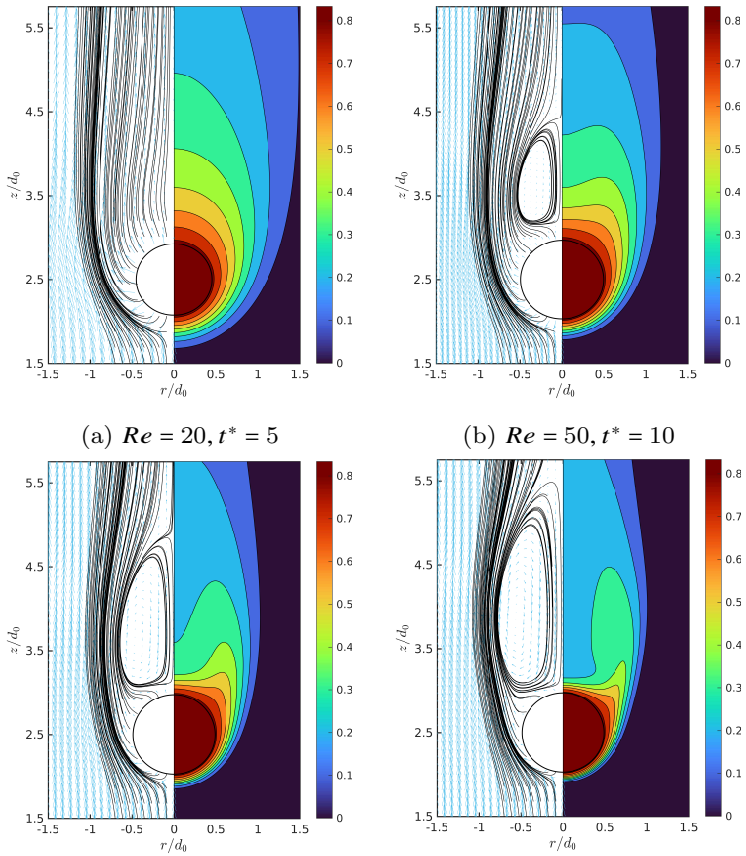

(a) $Re = 20, t^* = 5$ (b) $Re = 50, t^* = 10$

(c) $Re = 100, t^* = 20$ (d) $Re = 200, t^* = 30$

$We = 0.65, B_M = 5$

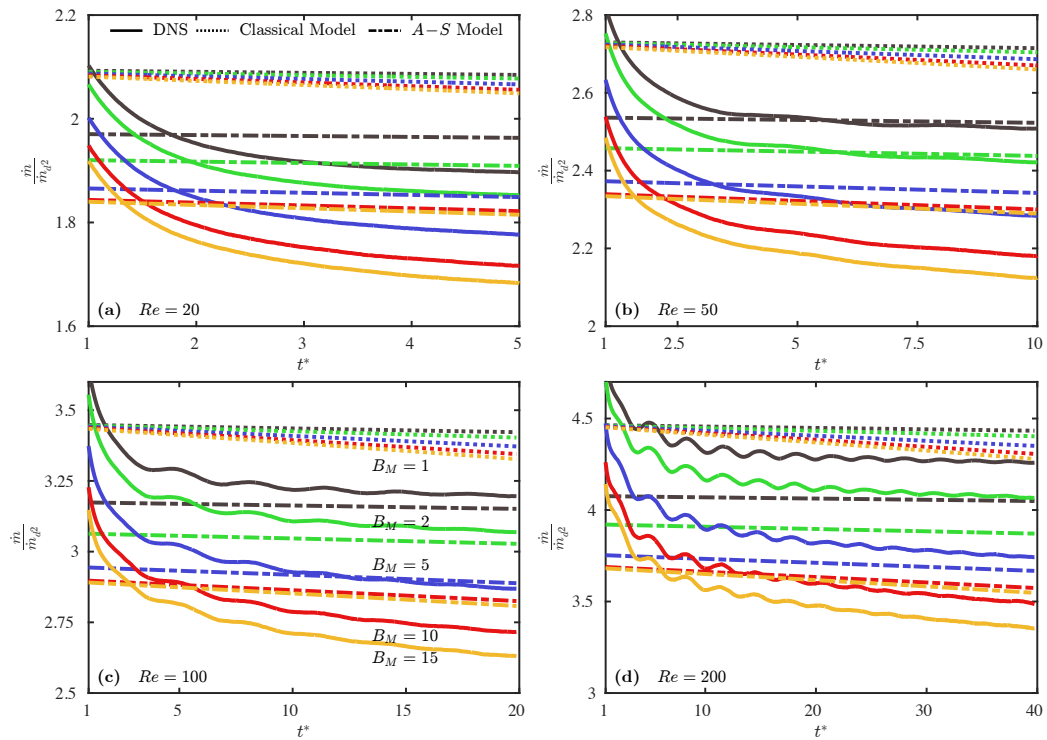

- The classical model overpredicts evaporation rate
- The Abramzon-Sirignano model outperforms the classical model

Nearly Spherical Droplet: Effects of Reynolds Number

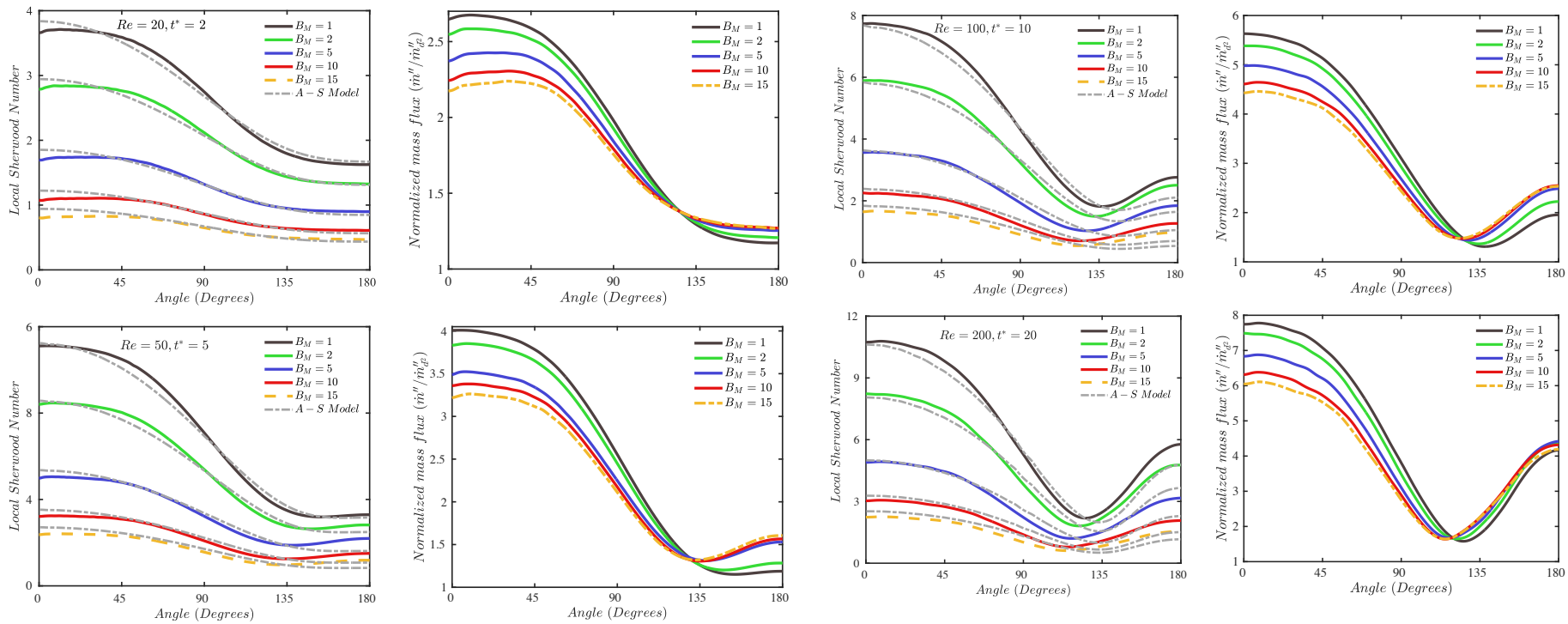

$We = 0.65$

- The Abramzon-Sirignano model performs well on the leading edge
- But significantly underpredicts on the trailing edge where boundary layer seperates

Nearly Spherical Droplet: Comparison with models

$We = 0.65$

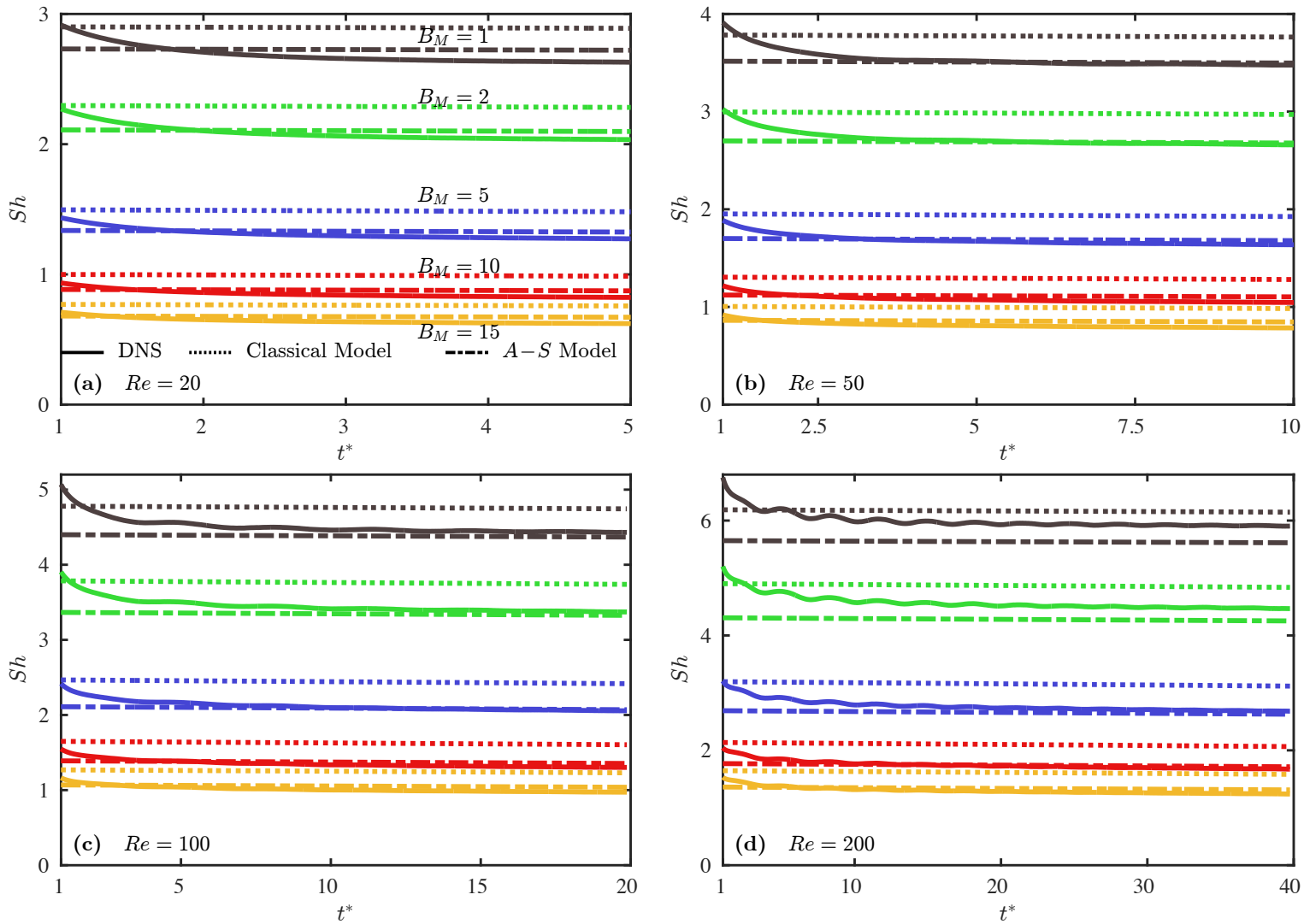

- The Abramzon-Sirignano model outperforms the classical model

Nearly Spherical Droplet: Comparison with models

$We = 0.65$

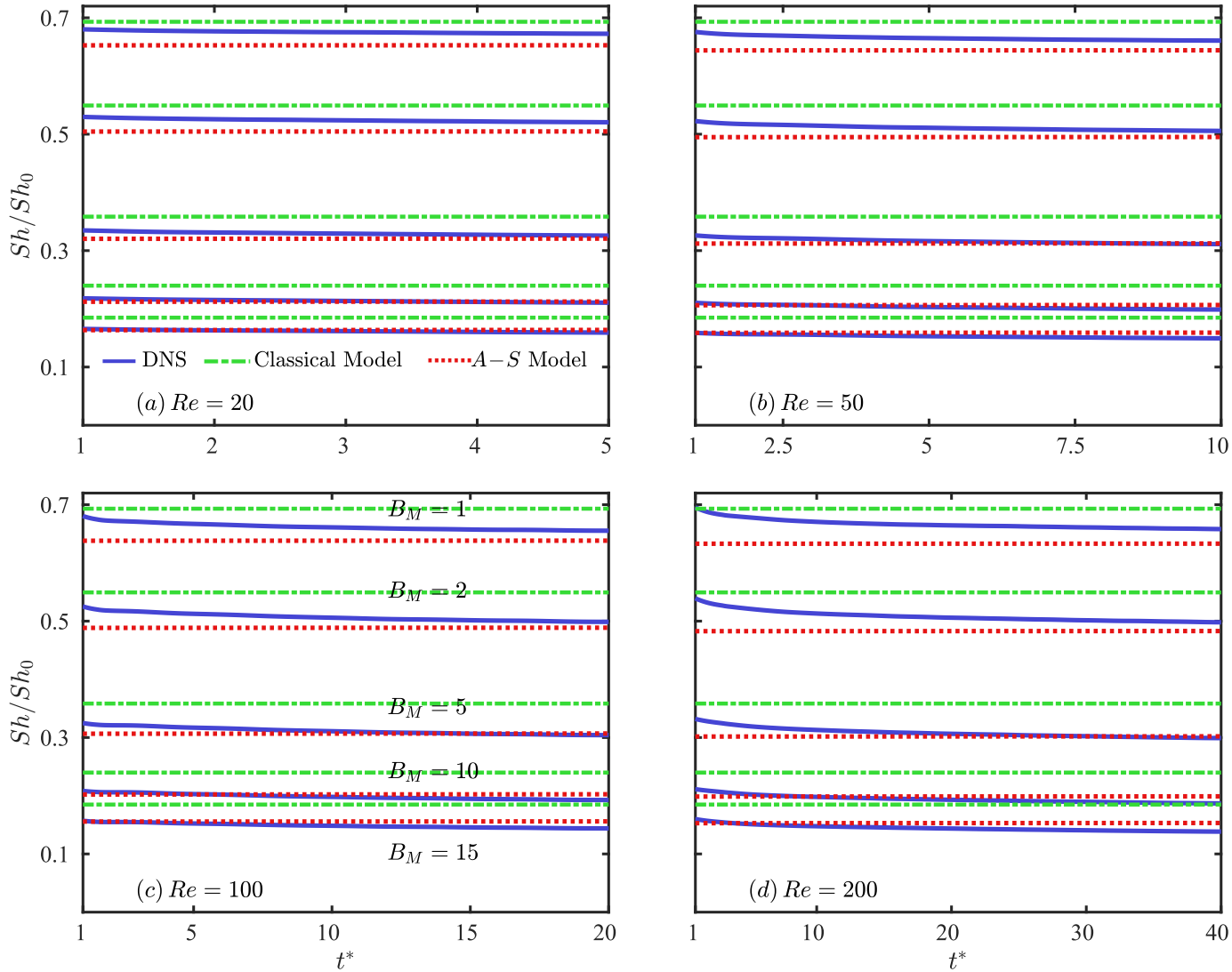

- The Abramzon-Sirignano model outperforms the classical model

Nearly Spherical Droplet: Comparison with models

$We = 0.65$

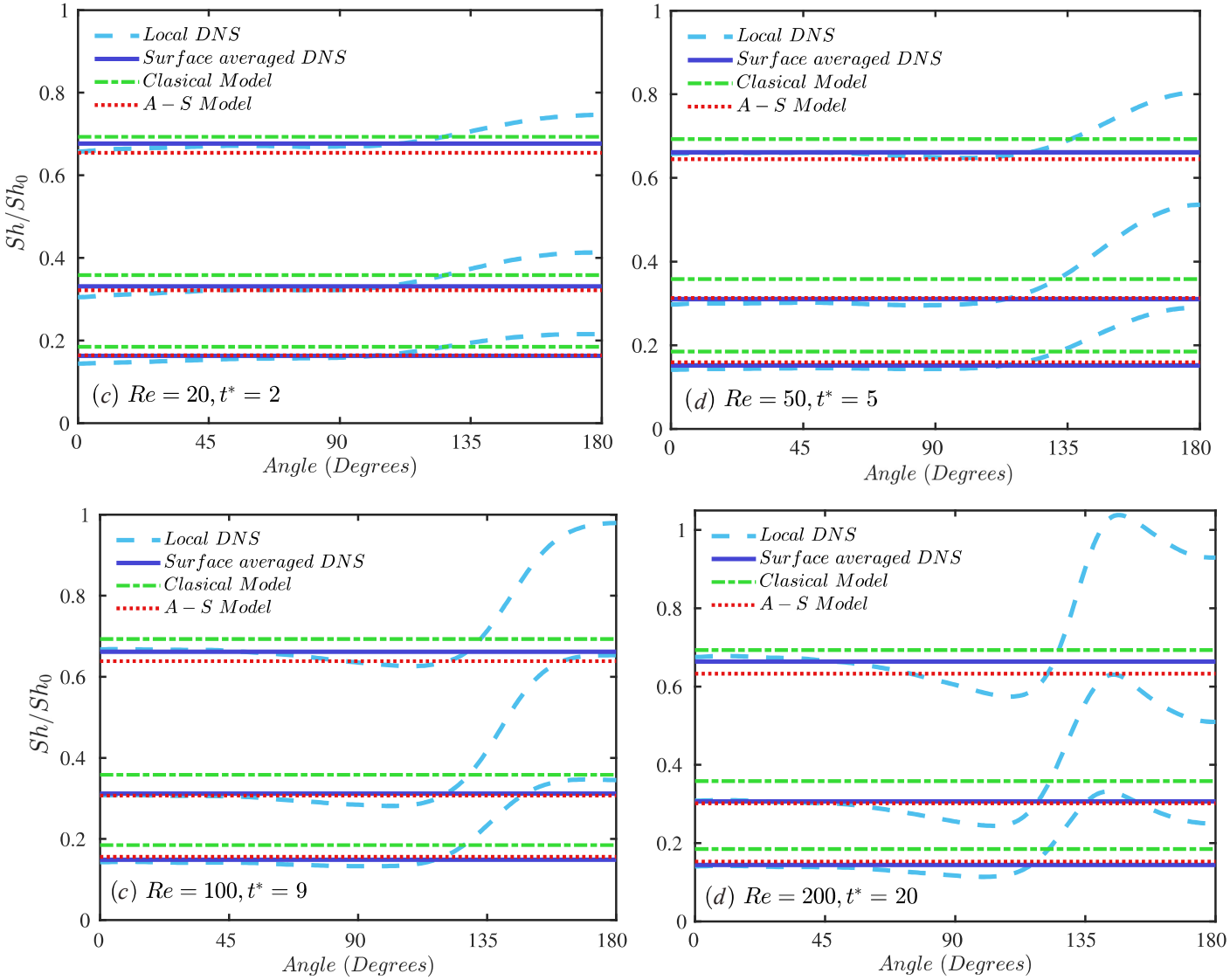

- The low order models perform poorly in the after BL separation

Nearly Spherical Droplet: Comparison with models

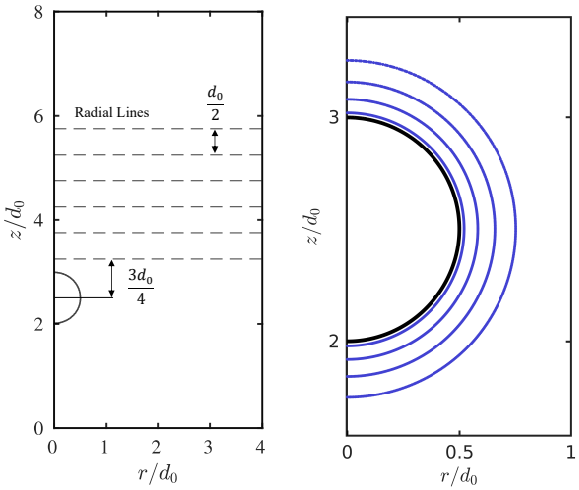

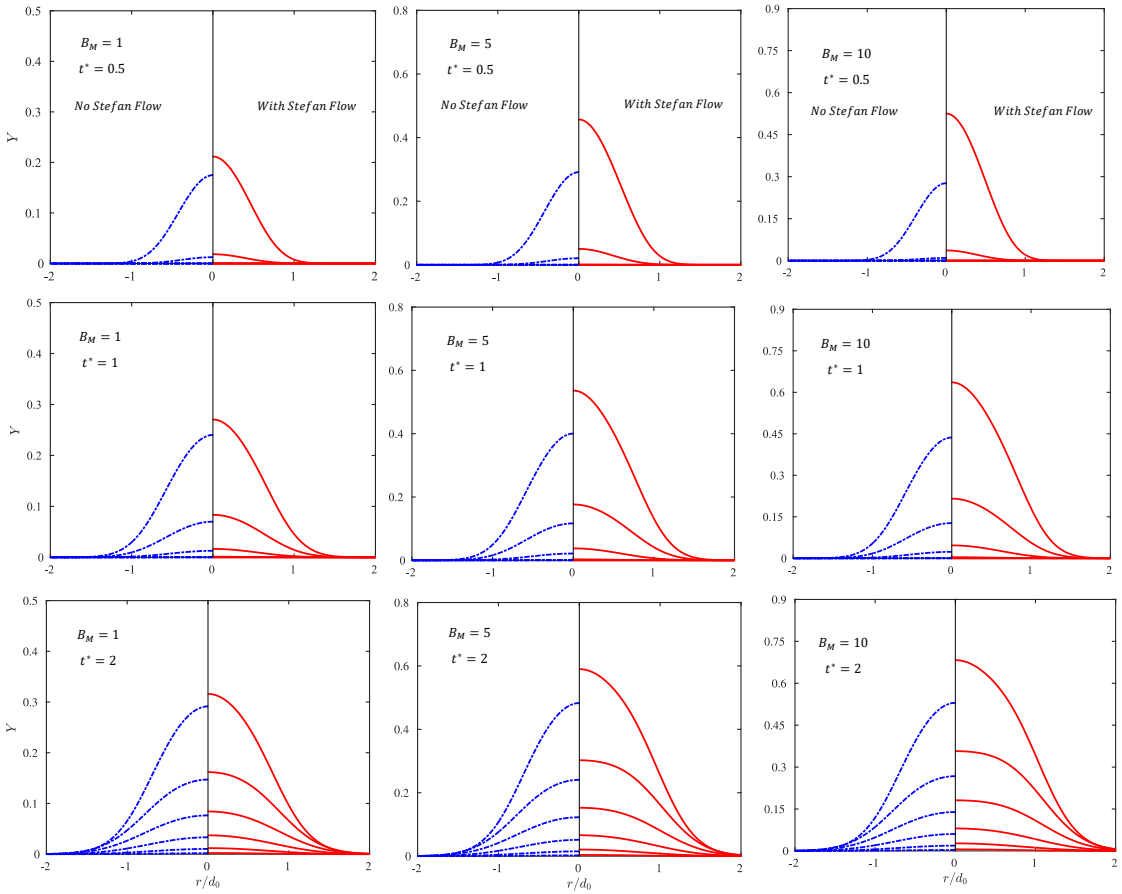

Figure 14: Mass fraction at designated radial lines in the wake of evaporating droplet($Re = 20$)

Nearly Spherical Droplet: Effects of Stefan Flow

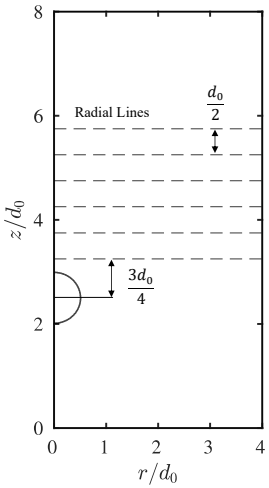

$Re = 20$

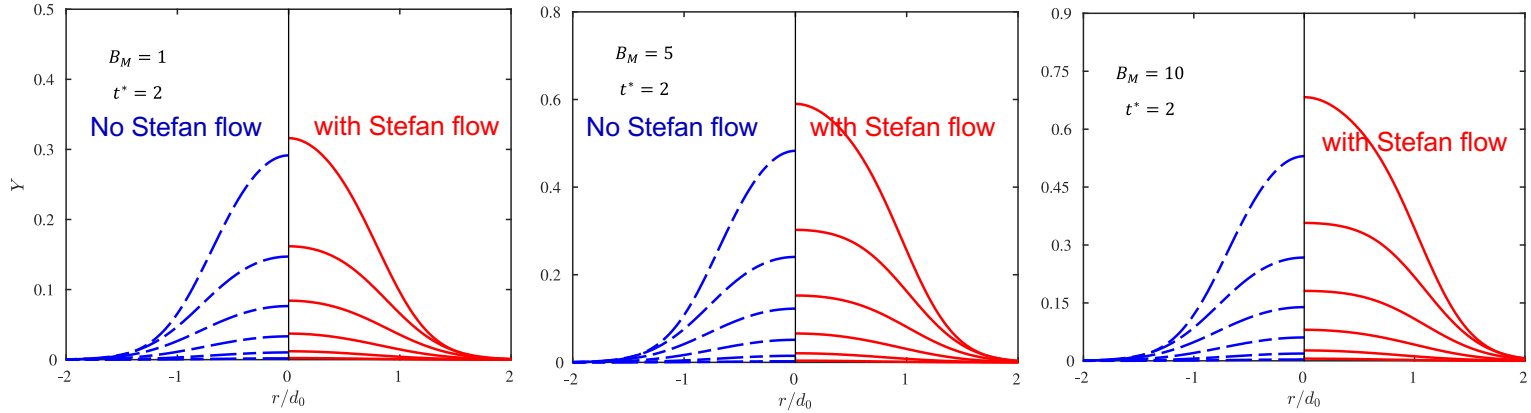

$Re = 100$

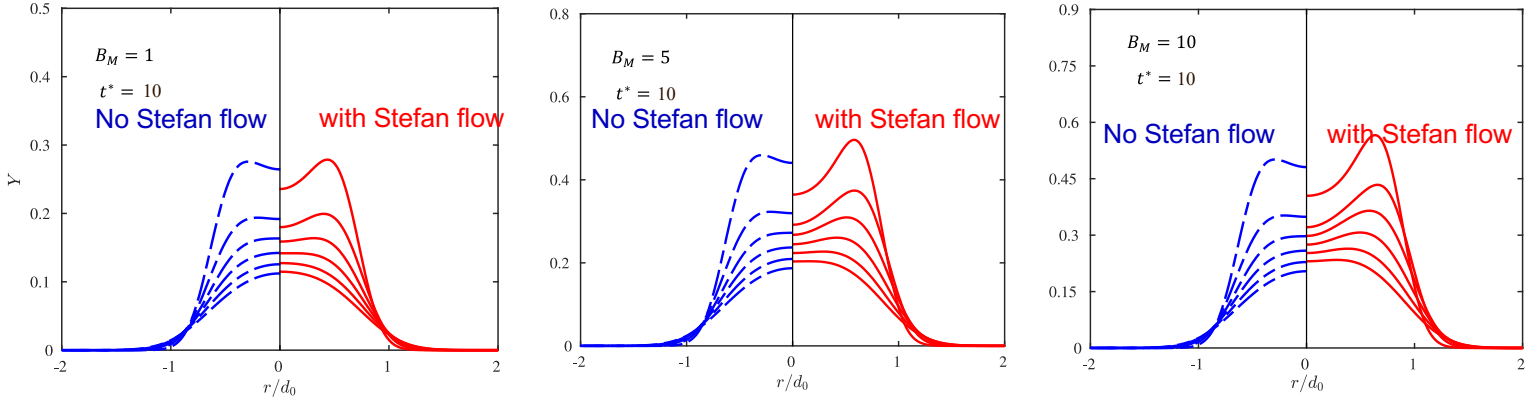

Effects of Deformation (We)

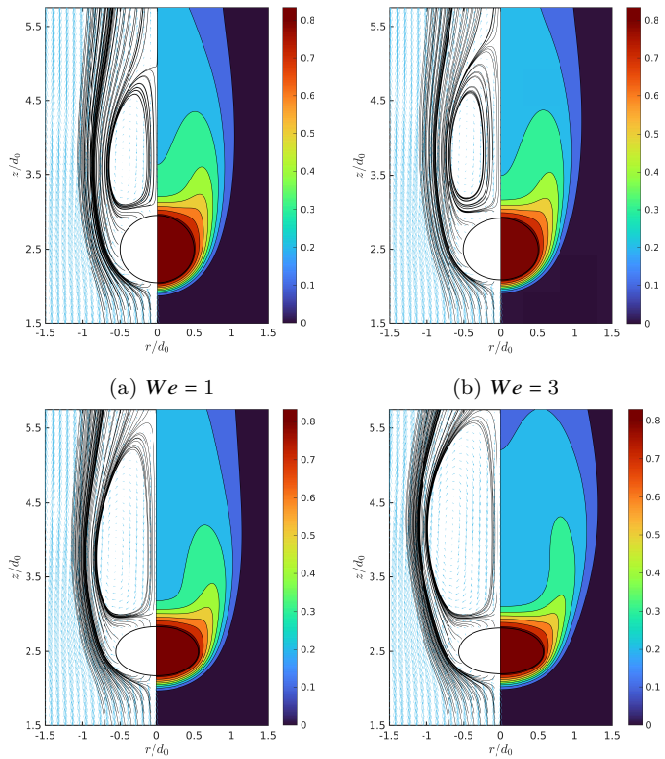

$B_M = 5, Re = 100, t^* = 15$

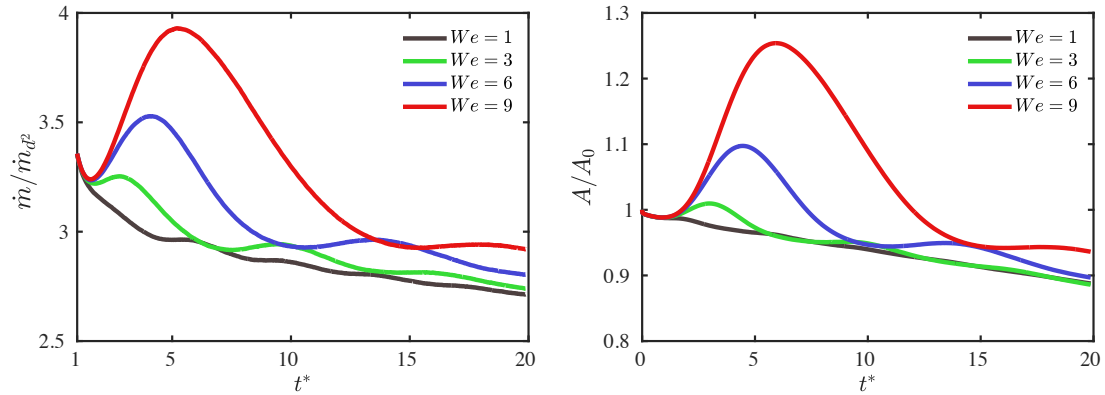

Temporal evolution of mass transfer rare (left) and surface area (right)

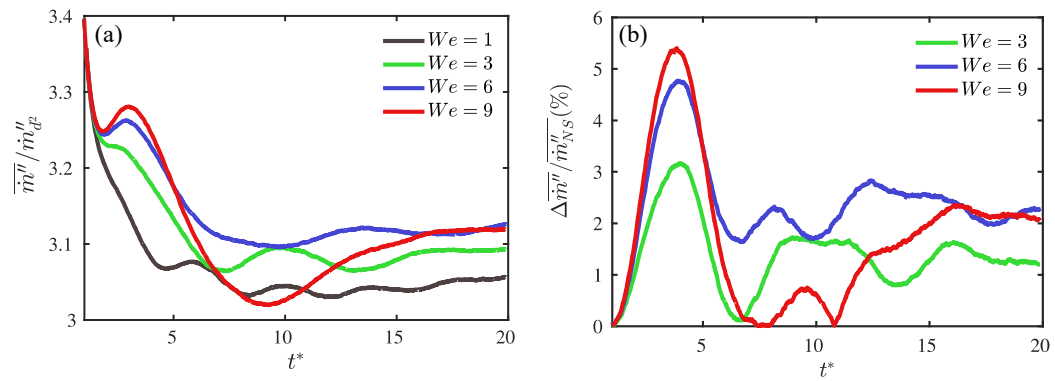

Surface-averaged mass flux (left) and percentage difference (right)

Evaporation rate strongly correlates with surface area

Effects of Deformation (We)

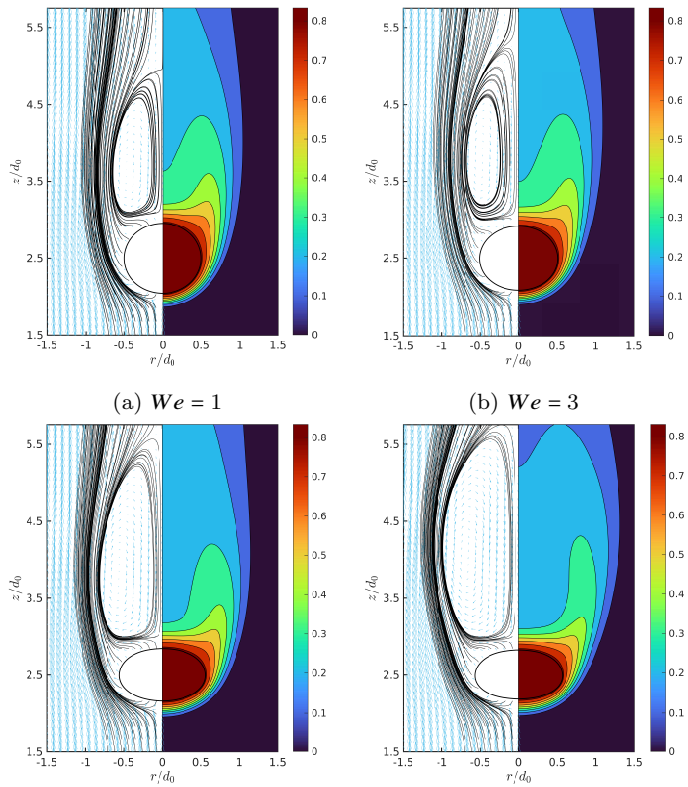

(a) $We = 1$ (b) $We = 3$ (c) $We = 6$ (d) $We = 9$

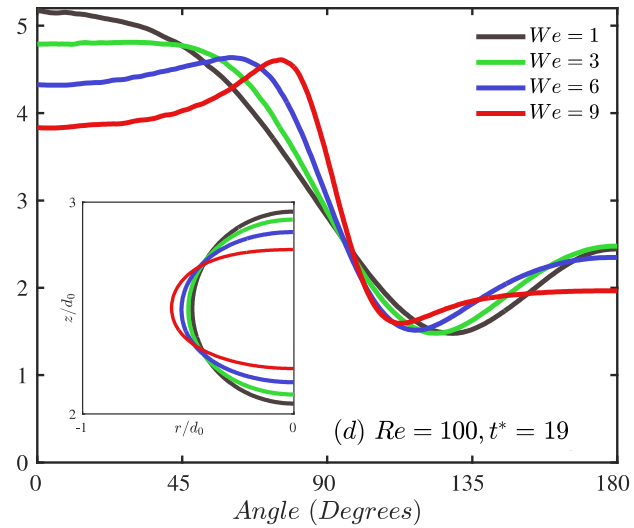

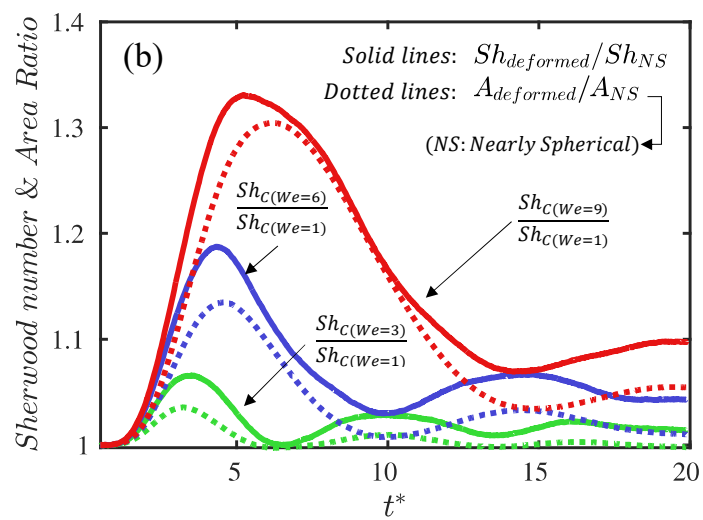

Evaporation rate strongly correlates with surface area

Conclusions

- The front-tracking method is presented for interface-resolved simulations of droplet evaporation
  - Distributing evaporative flux near droplet is computationally inexpensive but results in 1st order spatial accuracy
  - Hybrid method is more expensive but results in 2nd order spatial accuracy
  - Both methods are rigorously validated

- Extensive simulations are performed to examine droplet evaporation is convective environments
  - A thin mass boundary layer (BL) forms at the interface
  - Stefan flow thickens BL and results in early separation and larger recirculation zone, greatly influencing evaporation rate
  - The classical model outperforms Abramzon-Sirignano model at very low Re
  - But, Abramzon-Sirignano model performs much better for Re of practical interest
  - Droplet deformation greatly affects evaporation rate and must be incorporated in low order models. Evaporation rate correlates well with the deformation rate

- Future works:
  - Extension to full 3D (in progress)
  - Investigation of effects of turbulence
  - Investigation of effects of combustion

Viscoelasticity & Surfactant

Z, Ahmed, D. Izbassarov, J. Lu, G. Tryggvason, **M. Muradoglu**, O. Tammisola, “Effects of soluble surfactant on lateral migration of a bubble in a pressure driven channel flow ”, International Journal of Multiphase Flow 126, 103251 (2020).

Z. Ahmed, D. Izbassarov, P. Costa, M. Muradoglu, O. Tammisola , “Turbulent bubbly channel flows: Effects of soluble surfactant and viscoelasticity”, *Computers & Fluids* 212, 104717 (2021)

D. Izbassarov, Z. Ahmed, P. Costa, V. Vuorinen, O. Tammisola, **M. Muradoglu**, “Polymer drag reduction in surfactant-contaminated turbulent bubbly channel flows ”, *Physical Review Fluids* 6 (10), 104302 (2021)

H.U. Naseer, Z. Ahmed, D. Izbassarov, **M. Muradoglu**, “Dynamics and interactions of parallel bubbles rising in a viscoelastic fluid under buoyancy”, *Journal of Non-Newtonian Fluid Mechanics* 313, 105000 (2023)

H.U. Naseer, D. Izbassarov, Z. Ahmed, **M. Muradoglu**, “Lateral migration of a deformable fluid particle in a square channel flow of viscoelastic fluid”, *Journal of Fluid Mechanics* 996, A31 (2024)

H.U. Naseer, D. Izbassarov, M.E. Rosti, **M. Muradoglu**, “Bubbles-induced transition to elasto-inertial turbulence”, *Journal of Fluid Mechanics (submitted) (2025)* arXiv preprint arXiv:2503.03943

Viscoelastic/Elastoviscoplastic Fluids

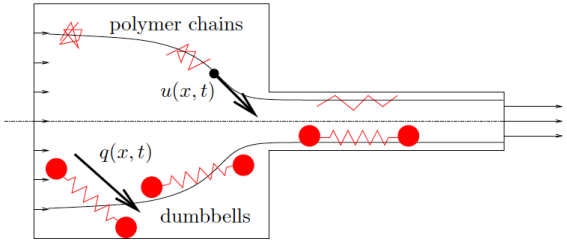

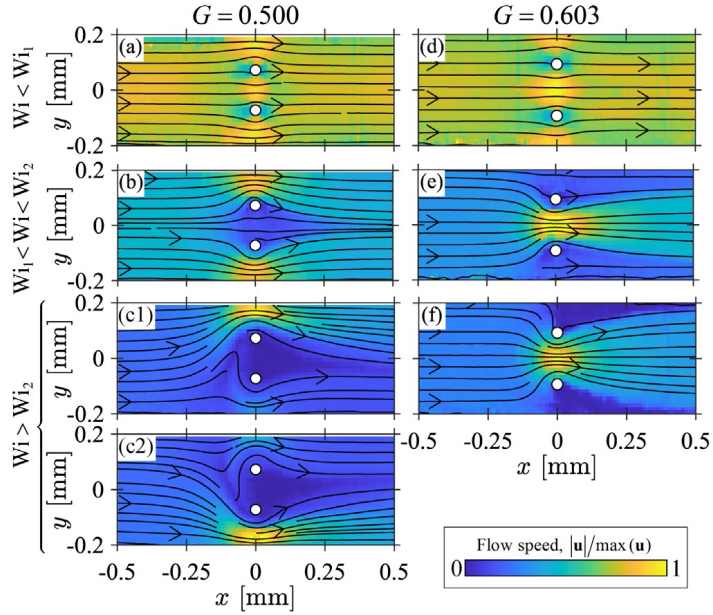

Hopkins et al. PRL, 126, 054501 (2021)

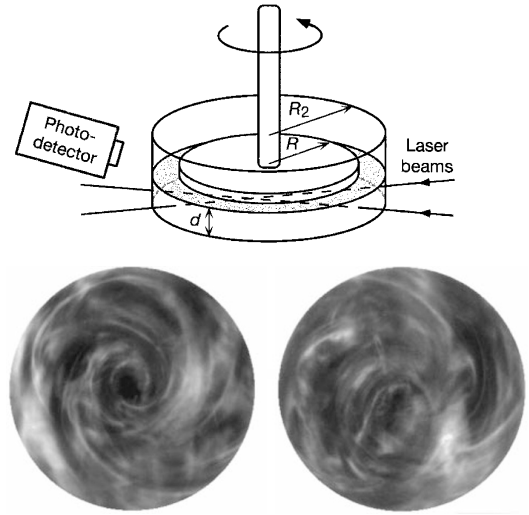

Groisman & Steinberg, Nature (2000)

Rod Climbing Effect

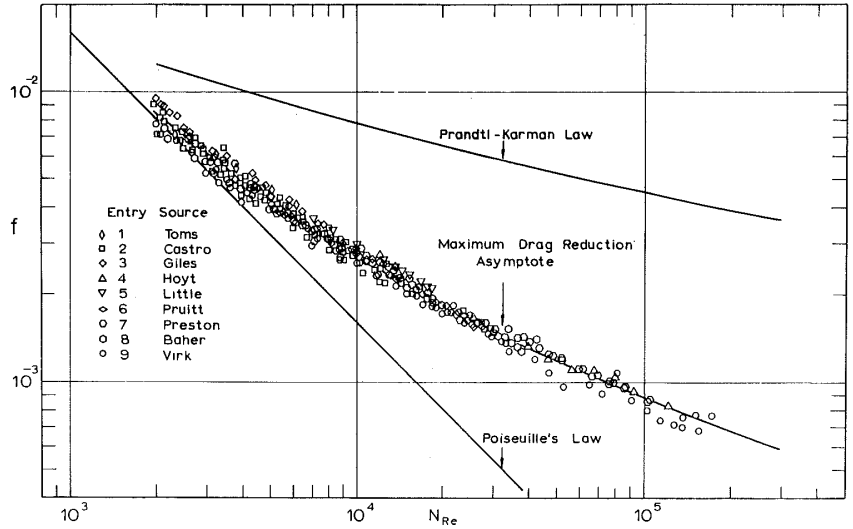

Virk et al. Trans. ASME (1970)

Surfactant

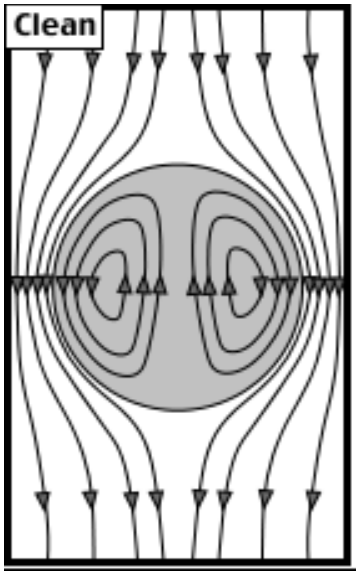

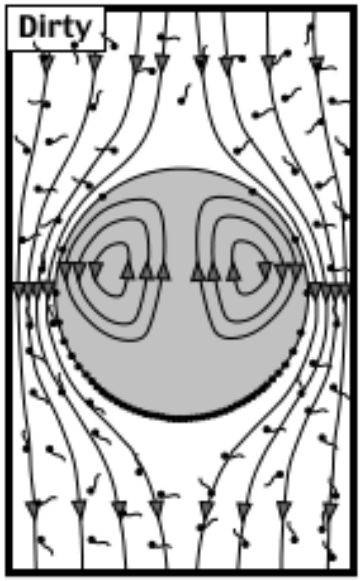

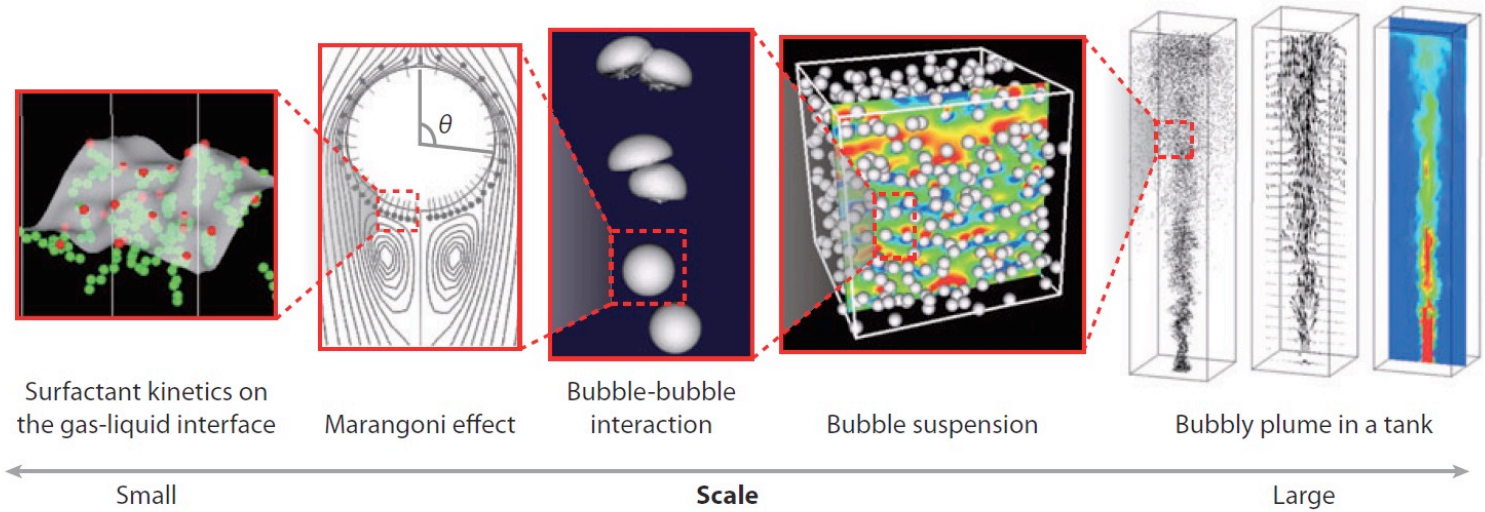

- Exists as impurities or added deliberately to the system
- Tend to collect at the interface and reduce surface tension
- Non-uniform surface tension induces **Marangoni** stresses
- A minute amount may change structure of a bubbly flow completely
- **A challenging task for simulations**

Mathematical Formulation

- **Incompressible Flow Equations: One-field formulation**

$$\frac{\partial \rho \mathbf{u}}{\partial t} + \nabla \cdot (\rho \mathbf{u}\mathbf{u}) = -\nabla p - \frac{dP_0}{d\nu}\boldsymbol{j} + (\rho - \rho_{avg})\mathbf{g} + \nabla \cdot \mu_s(\nabla \mathbf{u} + \nabla \mathbf{u}^T) + \nabla \cdot \boldsymbol{\tau}$$

$$+ \int_A [\sigma(\Gamma)\kappa \mathbf{n} + \nabla_s \sigma(\Gamma)]\delta(\mathbf{x} - \mathbf{x_f})dA$$

viscoelastic stresses

$$\nabla \cdot \mathbf{u} = 0$$

- **Langmuir Equation of state**

$$\sigma(\Gamma) = \sigma_s[\max(\epsilon_\sigma, 1 + \beta_s \ln(1 - \frac{\Gamma}{\Gamma_\infty}))]$$

- **Surfactant concentration at interface (Stone 1990)**

$$\frac{D\Gamma A}{Dt} = AD_s \nabla_s^2 \Gamma + \dot{S}_\Gamma \qquad \dot{S}_\Gamma = k_a C_s(\Gamma_\infty - \Gamma) - k_d \Gamma$$

$$\nabla_s = \nabla - \mathbf{n}(\mathbf{n} \cdot \nabla)$$

- **Bulk surfactant concentration**

$$\frac{\partial C}{\partial t} + \nabla \cdot (C\mathbf{u}) = \nabla \cdot (D_{co}\nabla C) + \dot{S}_c$$

- **Viscoelasticity: FENE-P Model** (Bird et al. 1980; Izbassarov and Muradoglu, 2015)

$$\frac{\partial \boldsymbol{A}}{\partial t} + \nabla \cdot (\boldsymbol{u}\boldsymbol{A}) - (\nabla \boldsymbol{u})^T \cdot \boldsymbol{A} - \boldsymbol{A} \cdot \nabla \boldsymbol{u} = -\frac{1}{\lambda}\left(\frac{\boldsymbol{A}}{1 - \mathrm{trace}(\boldsymbol{A})/L^2} - \boldsymbol{I}\right)$$

$$\boldsymbol{\tau} = \frac{\mu_p}{\lambda}\left(\frac{\boldsymbol{A}}{1 - \mathrm{trace}(\boldsymbol{A})/L^2} - \boldsymbol{I}\right)$$

Effects of surfactants (Takagi et al. 2011)

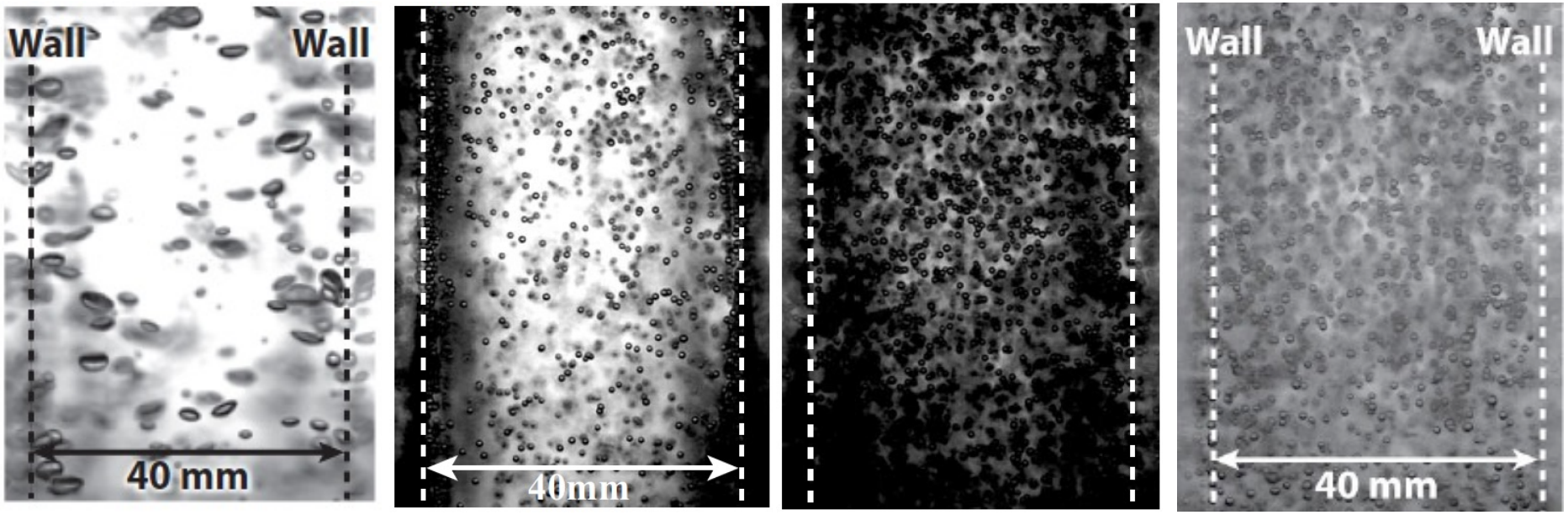

Clean water | 42 ppm 3-pentanol | 168 ppm 3-pentanol | 2 ppm TritonX-100

- Clean water case: Bubbles coalesce and become deformable
- 42 ppm 3-pentanol (little surfactant): Bubbles do not coalesce and tend to collect near the wall
- 168 ppm 3-pentanol: Bubbles are distributed more uniformly across the channel
- Only 2 ppm of TritonX-100 surfactant produce same results as 168 ppm of 3-pentanol surfactant type

Effects of surfactants: Single Bubble (Ahmed et al. 2020)

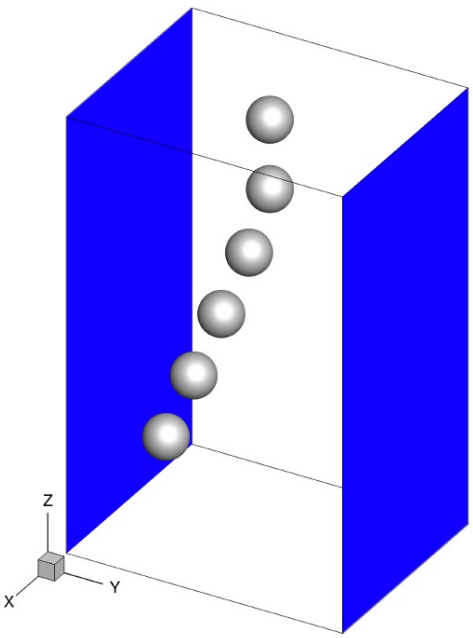

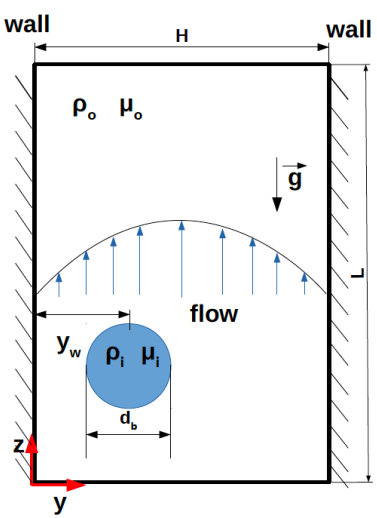

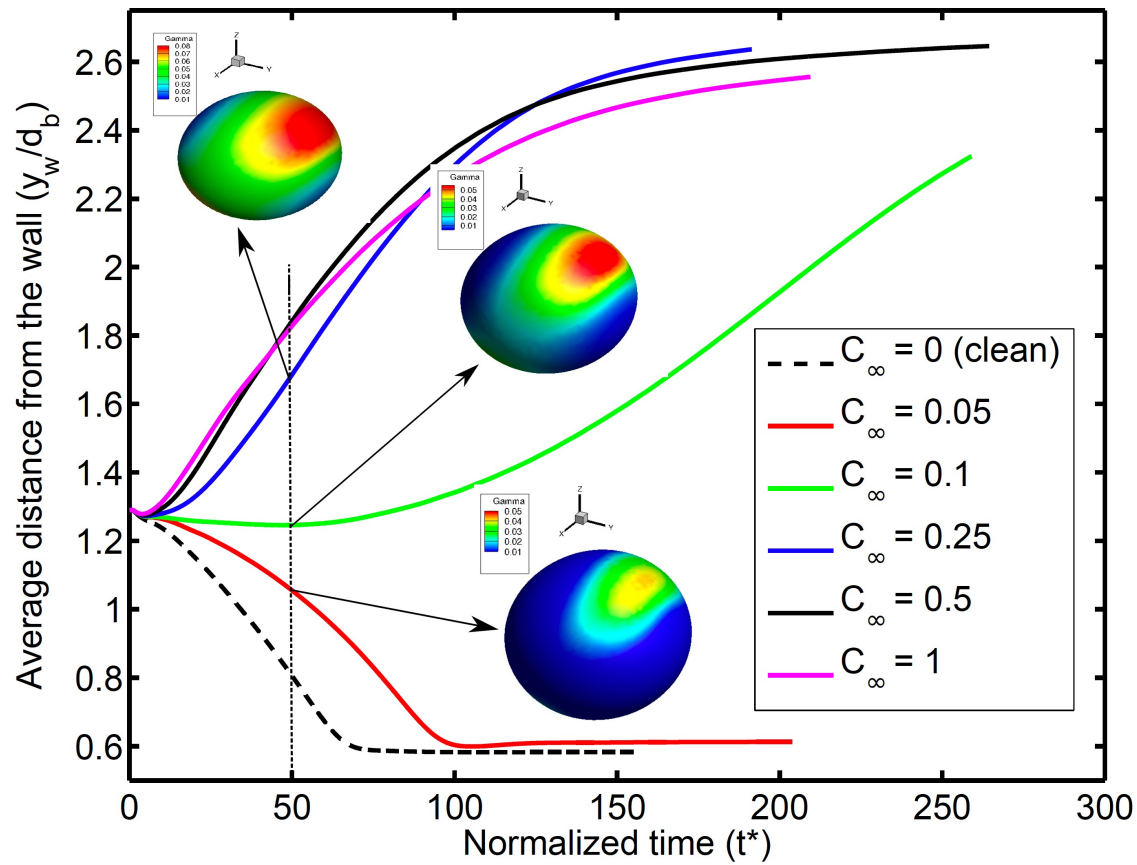

$$Re_c = 1000, \beta_s = 0.5, Pe_s = Pe_c = 200, Bi = 1.2$$

Ahmed et al., IJMF (2020)

Effects of surfactants: Newtonian Bubbly Flow ($Re_\tau = 180$)

Bubble distribution and flow structure

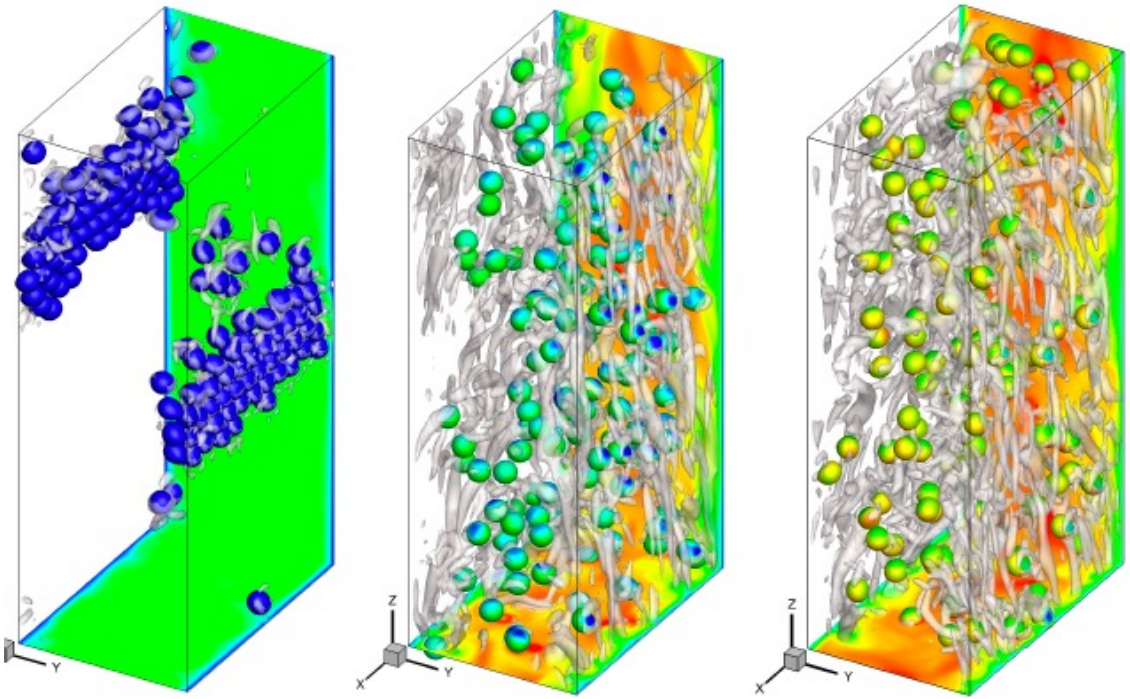

$C_\infty = 0$ ppm (clean) | $C_\infty = 0.25$ ppm (Cont.) | $C_\infty = 0.5$ ppm (Cont.)

Flow Rate

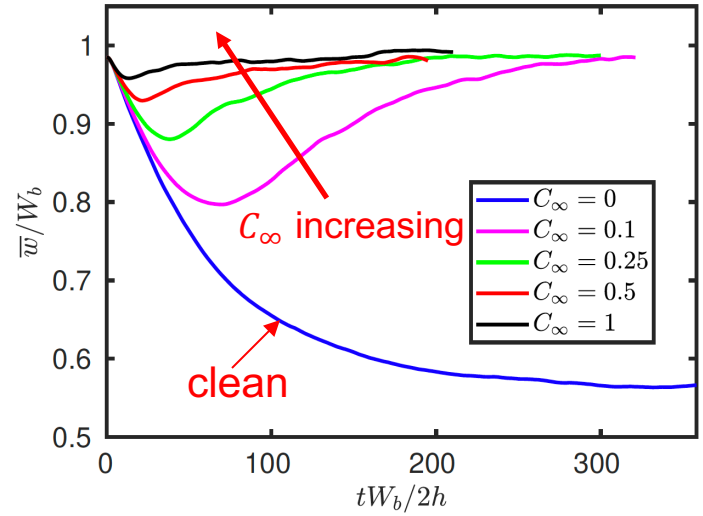

(b) $Re_\tau = 180$

Surfactant: Triton X-100
All Newtonian ($Wi = 0$)

- Even a tiny amount of TritonX-100 alters the structure of the turbulent bubbly flow dramatically
- Qualitatively in good agreement with the experimental observations of Takagi et al. 2008

Multiphase flows: Drag Reduction by polymer additives

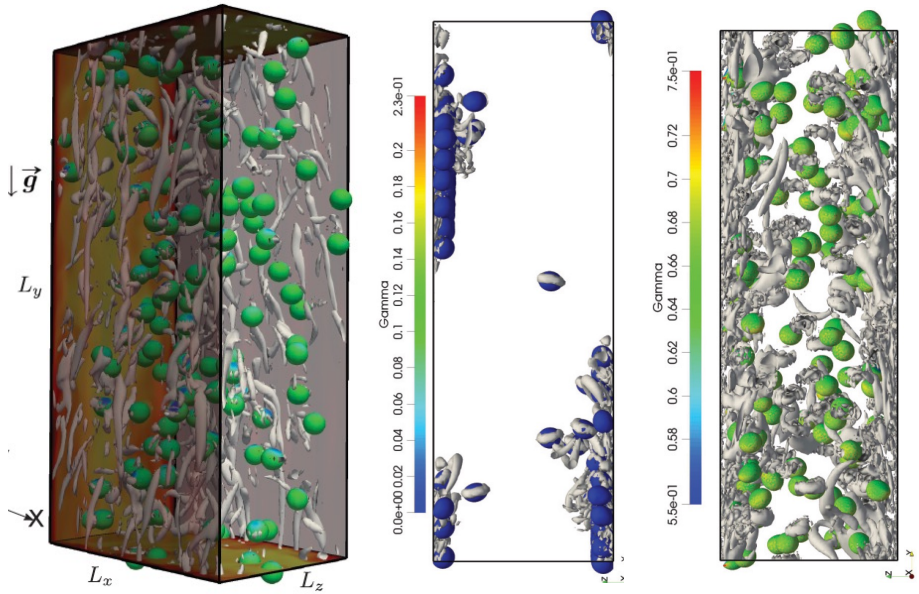

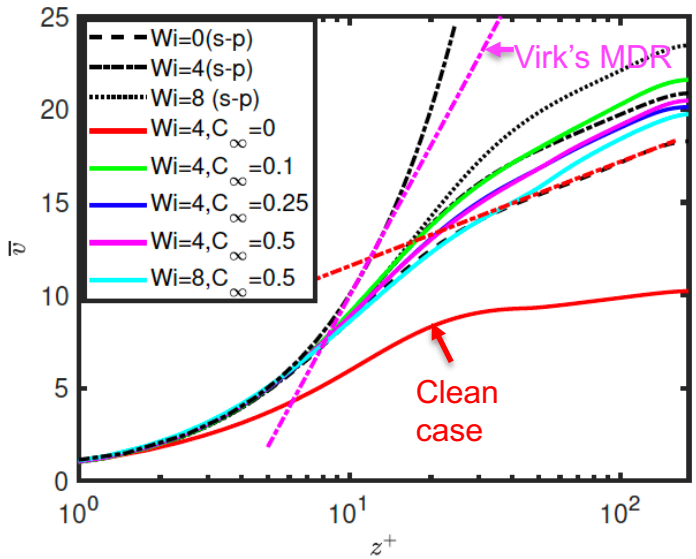

Ahmed et al. Phys. Rev. Fluids, 6, 104302 (2021)

- Interface-resolved DNS of turbulent bubbly channel flow at $Re_\tau = 180$
  - Polymer additives (FENE-P)
  - Soluble surfactant (Triton-X100)
- Main Findings:
  - Drag reduction is fully realized in single-phase flow
  - Drag reduction is lost in bubbly flows due to formation of bubble wall layer
  - Polymer drag reduction is realized only when surfactant is present

Elastic instability

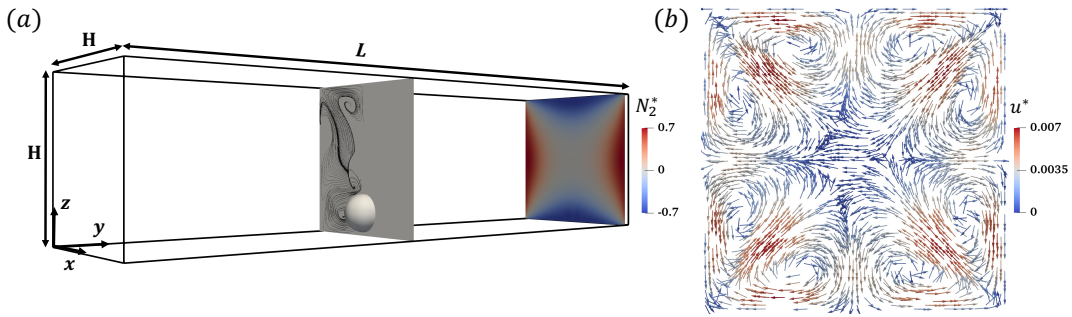

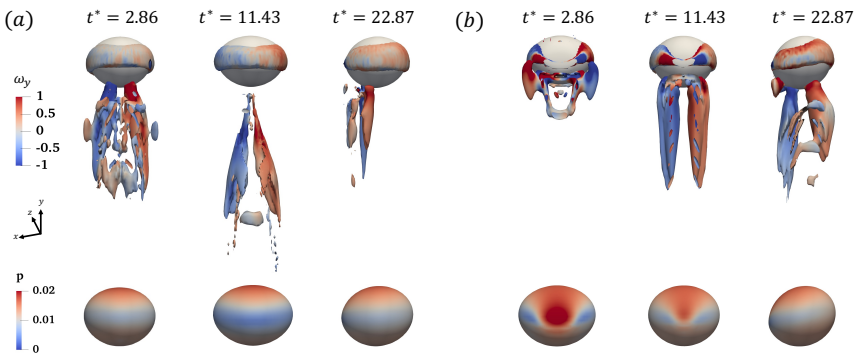

$(a)\ \alpha = 0 \quad (b)\ \alpha = 0.1$

- A single bubble in pressure-driven channel (Giesekus fluid)
  - Elastic instability caused by the curvature of the bubble
  - A secondary flow develops at a significant shear-thinning
  - Shear thinning reduces and eventually suppresses the elastic instability
- Many bubbles (preliminary results)
  - More complex flow but not turbulent yet
  - Conditions for triggering transition to turbulence (under investigation)

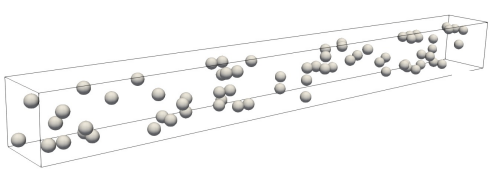

Computational domain with bubbles ($vf = 3\%$)

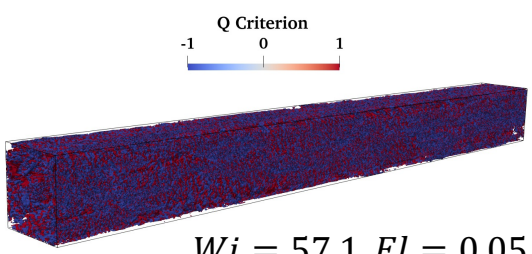

$Wi = 57.1, El = 0.05$

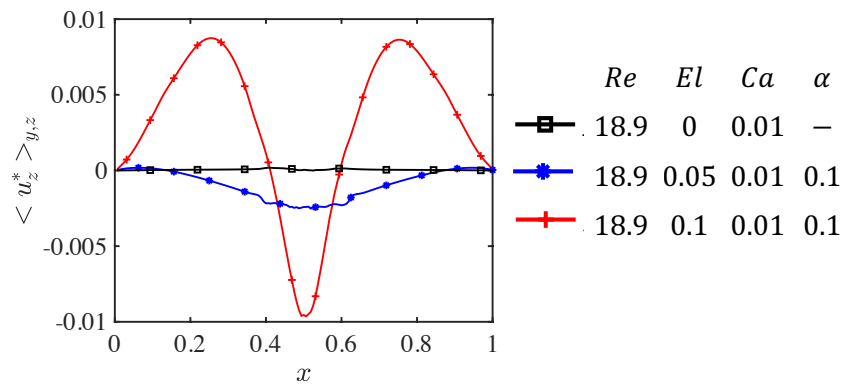

(Secondary flow)

Naseer et al. JFM, 996, A31 (2024)

Bubble-Induced instability & Transition to Turbulence

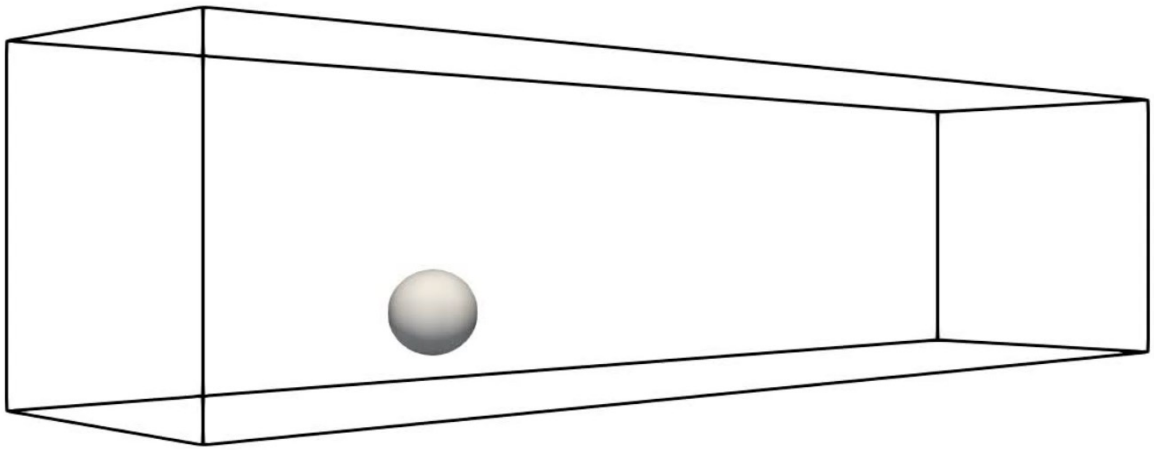

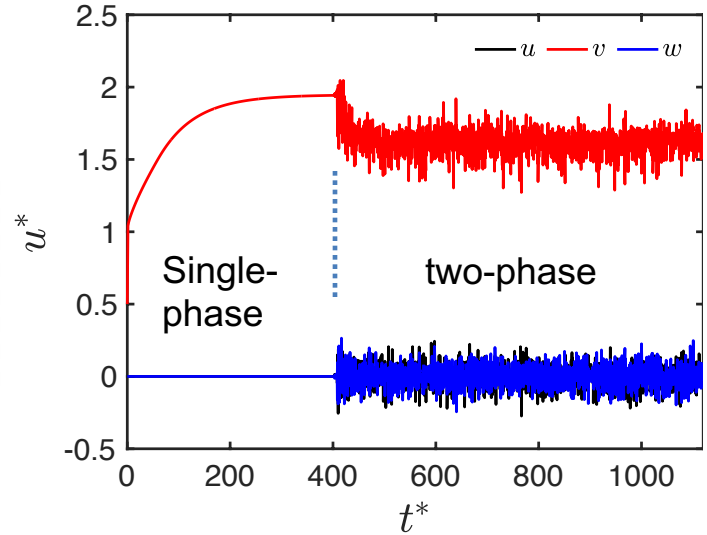

Naseer et al. JFM (submitted) (2025)

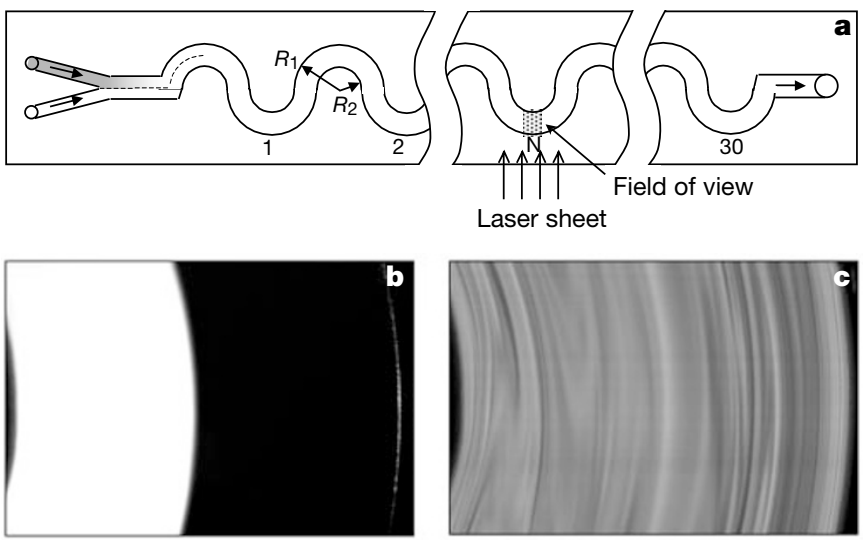

Groisman & Steinberg, Nature (2001)

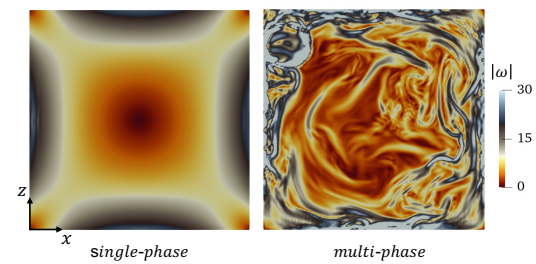

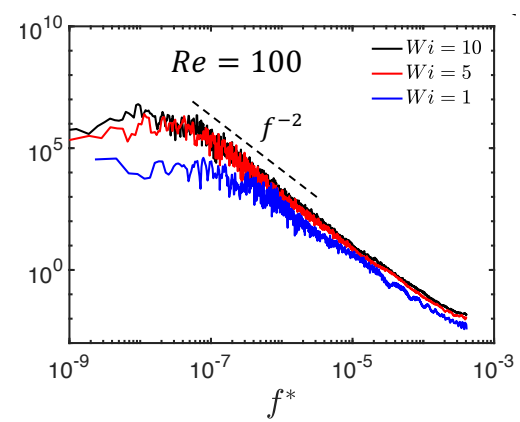

Thanks

- Supported by The Scientific and Technical Council of Turkey (TUBITAK) and Turkish Academy of Sciences (TUBA)

- Collaborators:
  - Prof. Howard A. Stone, Princeton University
  - Prof. Gretar Tryggvason, Johns Hopkins University
  - Prof. James B. Grotberg, The University of Michigan, Ann Arbor
  - Prof. Utkan Demirci, Stanford University
  - Prof. Alper Kiraz, Koc University